Mechanical and Psychophysical Studies of Surface Wave Propagation during Vibrotactile Stimulation

by

Katherine O. Sofia

B.S. Mechanical Engineering
Union College, 2010

SUBMITTED TO THE DEPARTMENT OF MECHANICAL ENGINEERING IN PARTIAL FULFILMENT OF THE REQUIREMENTS FOR THE DEGREE OF

MASTER OF SCIENCE IN MECHANICAL ENGINEERING

AT THE
MASSACHUSETTS INSTITUTE OF TECHNOLOGY

JUNE 2012

Signature of Author_____
Department of Mechanical Engineering
May 11, 2012

Certified by_____
Lynette A. Jones
Senior Research Scientist in Mechanical Engineering
Thesis Supervisor

Accepted by_____
David E. Hardt
Chairman, Department Committee on Graduate Students

Mechanical and Psychophysical Studies of Surface Wave Propagation during Vibrotactile Stimulation

by
Katherine O. Sofia

Submitted to the Department of Mechanical Engineering
on May 11, 2012 in partial fulfillment of the
requirements for the Degree of Master of Science in
Mechanical Engineering

Abstract

Vibrotactile displays are based on mechanical stimulation delivered using an array of motors to communicate with the user. The way in which the display's motors are spaced and positioned on the body can have a significant impact on the effectiveness of communication, especially for tactile displays used to convey spatial information. The objective of the present research was to determine how the surface waves induced by vibrotactile stimulation of the skin varied as a function of the site on the body where the motors were mounted, and how these waves influenced the ability to localize vibrotactile stimulation. Three locations on the body were selected for study: the palm, the forearm, and the thigh. A flexible printed circuit board containing 3-axis micro-accelerometers was fabricated to measure the amplitude and frequency of surface waves produced by a vibrating motor at each body site. Results of these experiments showed significant differences in the frequency and amplitude of vibration on the glabrous skin on the palm as compared to the hairy skin on the arm and thigh. The palm had the highest frequency and lowest amplitude surface waves, and the forearm and thigh were very similar with lower frequency higher amplitude surface waves. No anisotropies were found from surface wave measurements. Most wave attenuation occurred within the first 8 mm from the motor, but there were still detectable amplitudes at a distance of 24 mm from the motor, which suggests that motor spacing should be at least 24 mm for this type of motor when used for precise spatial localization.

A series of psychophysical experiments was conducted using a three-by-three array of motors in which the ability of subjects to localize the point of stimulation in an array was determined at each of the three body locations. The results from these experiments indicated that the palm had the highest localization accuracy (81% correct) as compared to the forearm and thigh which had similar localization accuracies (49% correct on forearm, 45% correct on thigh). Accuracy on the palm and forearm improved when the motor spacing increased from 8 mm to 16 mm, but increased spacing did not improve accuracy on the thigh. The results also showed that subjects were more able to identify the column of activation as opposed to the row of activation, which suggests a higher spatial acuity along the medial-lateral as opposed to proximal-distal axis. The localization experiments indicate that glabrous skin is better suited for precise spatial localization than hairy skin, and that precise spatial localization requires an inter-motor spacing of more than 16 mm at these sites.

Thesis Supervisor: Lynette A. Jones
Title: Senior Research Scientist

Acknowledgements

I would first like to thank my advisor, Dr. Lynette A. Jones for taking me on as a research student and for advising and supporting me in my research. Without her help and guidance I would never have been able to complete my research. Along with Lynette I would also like to thank the rest of the members of the BioInstrumentation lab for supporting me in my research by providing technical help as well as general feedback and advice. I would also like to thank all eleven of my willing and patient research participants for generously donating their time to me, without whom my research would not have been possible.

Finally I would like to thank my family and friends for always supporting me and believing in me, and for listening to me vent about my frustrations with research. Your support and encouragement is what kept me going. Dad, thank you for encouraging me to apply to MIT in the first place. I never thought I could do this. I owe my success to you.

This research was funded in part by the National Science Foundation.

Table of Contents

1. Introduction

The skin is the most expansive organ in the human body containing thousands of receptors all responsible for transmitting the essential sense of touch. When other senses are compromised such as vision or hearing, our skin's senses can be used in substitution. This is the concept behind tactile displays. Tactile displays are devices that can transmit information to a person through the sense of touch. Tactile displays can be used in many applications and come in varying forms. While some displays use static stimuli such as the stationary patterns of bumps used in Braille, others use dynamic stimuli such as vibrating motors contained within a wearable device such as a belt, vest, or glove (Chen et al., 2008; Jones & Held, 2008; Jones et al., 2009; Salzer et al., 2010). The latter is known as a vibrotactile display, since this method uses vibration to communicate. Vibrotactile displays commonly comprise a series of small vibrating motors mounted on the skin that vibrate in defined patterns to communicate information to the wearer. While tactile displays can be an effective method of communication, in order to improve the usefulness of tactile displays, designers must consider the body's sensing capabilities and how the nervous system will react to the stimuli provided by such displays.

All sensations of touch are communicated and governed by four factors: modality, location, intensity and timing (Gardner & Martin, 2000). Modality refers to the way in which a particular stimulus is received by the body based on the type of energy it transmits and which receptors are activated by that energy. Location is also determined by the set of sensory receptors activated that indicate the position and size of a stimulus on the body depending on their placement and density within the skin. The intensity and timing of stimulation are both based on the firing characteristics of the activated sensory neurons. Intensity is controlled by the firing rates of the stimulated receptors, while timing is simply governed by the duration of stimulation, beginning from the time of initial receptor firing until firing stops. Therefore, both intensity and timing are controlled by how quickly the activated receptors react to a stimuli or how quickly they can engage and disengage a response (Gardner & Martin, 2000). When considering all this in relation to designing tactile displays two key issues must be considered: which types of receptors—slowly adapting or rapidly adapting receptors—are being activated by given stimuli based on body location and stimulus type, and next, how can the stimuli be tailored to best activate those receptors.

Much research has gone into examining the sensory properties and capabilities of skin (Bolanowski et al., 1994; Johansson & Vallbo, 1979; Konietzny & Hensel, 1977; Morioka et al., 2008; Stevens & Choo, 1996), as well as looking at the physical dynamic behavior of skin in response to an applied dynamic stimulus (Boyer et al., 2007; Franke et al., 1951; Jones & Held, 2008; Li et al., 2011; Liang & Boppart, 2010). The goal of the present research is to examine how the skin responds to vibrotactile stimulation with the objective of determining what the optimal configuration of vibrotactile displays is at different locations on the body, when they are used for spatial cuing.

2. Background

2.1 Skin Sensory Properties

The somatosensory system responsible for detecting touch receives its input from cutaneous mechanoreceptors. More specifically, the dorsal root ganglion neurons are the sensory neurons responsible for conveying information to the spinal cord and brain regarding the sense of touch. The axons of dorsal root ganglion neurons are known as afferents and they relay sensory information from the periphery to the central nervous system. Each afferent unit ends as either a free nerve ending or a mechanoreceptor (encapsulated nerve ending). The bare nerve endings respond to sensations of temperature and pain, whereas mechanoreceptors sense mechanical stimuli that indent or otherwise deform the skin (Gardner et al., 2000). These mechanoreceptors sense the stimuli delivered by tactile displays.

2.1.1 Mechanoreceptors Present in Glabrous Skin

Glabrous skin, present on the lips, palms of the hands, and soles of the feet, is characterized by its hairless ridged nature, and contains four types of mechanoreceptive units: rapidly adapting type I (RA I) and type II (RA II or PC) and slowly adapting type I (SA I) and type II (SA II) (Johansson & Vallbo, 1979). These four types of mechanoreceptors terminate with different end-organs: Meissner's corpuscles (RA I), Merkel disks (SA I), Pacinian corpuscles (RA II), and Ruffini endings (SA II). The type I and type II is used to refer to the size of their receptive fields (the area of skin that excites a sensory neuron), where type I receptors have a small receptor field and type II have a large field. Rapidly adapting receptors respond quickly to changes in stimuli by producing quick short bursts of action potentials at the beginning and end of a stimulus. Slowly adapting receptors respond gradually to new stimuli, but will remain steadily active for an extended amount of time over the duration of stimulus contact. The Meissner's corpuscles (RA I) and Pacinian (RA II) corpuscles are rapidly adapting receptors that respond to rapid skin indentation such as vibration, but do not sense continuous pressure. Conversely the Merkel disks (SA I) and Ruffini endings (SA II) are slowly adapting receptors that only respond to steadily compressed nerve endings such that occurs from skin stretch when grasping an object (Gardner et al., 2000).

These four receptors are found among the superficial layers of skin and the deeper layers of the dermis and subcutaneous tissue. The sensing ability of each of these mechanoreceptors is partially

influenced by the size of their receptive fields. Meissner's corpuscles and the Merkel disk mechanoreceptors are located in the superficial layers of skin, at the junction between the dermis and epidermis, and have very small receptive fields ranging from 2 to 3 mm in diameter on the fingertip to about 10 mm in diameter on the palm (Gardner et al., 2000). Each of these small receptive fields contains about 10-25 Meissner's corpuscles or Merkel disk receptors and is attached to a single nerve ending, so that a single nerve fiber in the superficial layer collects information from many receptors at once, allowing these receptors to sense and communicate very fine detail. The Pacinian corpuscles and the Ruffini endings are located in the subcutaneous skin tissue, have much larger and less numerous receptive fields with less distinct edges allowing them to sense deeper more general deformations over broader areas of skin. This broader more general resolution is due to that fact that each of these receptor fields contains only one Pacinian corpuscle or Ruffini ending innervated by a single nerve fiber. Although the sensing resolution of these large receptor fields is generally less acute, each receptive field contains a smaller area of peak sensitivity located directly above the receptor (Gardner et al., 2000).

2.1.2 Mechanoreceptors Present in Hairy Skin

Hairy skin contains three of the same type of mechanoreceptors that are present in glabrous skin (Merkel disks, Pacinian corpuscles, Ruffini endings) as well as two other types of rapidly adapting mechanoreceptors: the hair follicle receptor and field receptors (Gardner et al., 2000). The hair follicle receptors respond to hair motion, whereas the field receptors are located around the joints and sense when the skin is stretched or rubbed (Gardner et al., 2000). Although hairy skin contains some of the same receptor types as glabrous skin, research suggests that these receptors may be arranged differently resulting in different sensory characteristics of the skin. As in glabrous skin, the Pacinian corpuscles and Ruffini nerve endings are located in the subcutaneous tissue of hairy skin, although less numerous and the Merkel disks are located closer to the superficial skin layers (the epidermal-dermal junction). Research has lead scientists to believe that not only are there fewer Pacinian corpuscles in hairy skin as compared to glabrous skin, but that they may also be more deeply imbedded in the tissue of hairy skin, contributing to reduced vibrational sensitivity (Bolanowski et al., 1994).

2.1.3 Variations in Mechanoreceptor Density with Body Location

The acuity and resolution of touch varies with body location due to variations in receptor density. Receptor density is inversely proportional to receptor field size, so for a given skin area, the smaller the receptor field size the greater the receptor density. Therefore, given that the glabrous skin on the hand

tends to have smaller receptor fields, it should be no surprise that glabrous skin also contains a relatively higher density of mechanoreceptors than hairy skin, making it easier to feel small details. However not all glabrous skin has a uniform receptor density, resulting in different sensitivity at different skin regions. Type 1 receptors (Meissner corpuscles and Merkel disks), which have small well defined receptive fields, vary greatly in density across glabrous skin surfaces. The type 2 receptors (Pacinian corpuscles and the Ruffini endings), which have larger less well defined receptor fields, are almost evenly distributed over a given area of glabrous skin. On the palmar side of the hand alone, which is covered entirely in glabrous skin, the nerve density, which is primarily dominated by Meissner and Merkel receptors, varies from 241 receptor units per square centimeter on the finger tips—the highest density of mechanoreceptive nerve fibers on the human body—to 95 units/cm^2 on the base of the fingers, to 58 units/cm^2 on the palm (Johansson & Vallbo, 1979). The receptor density on the hairy skin of the forearm and other limbs diminishes in a proximal to distal gradient, as "the peripheral parts of the extremities are...much more densely innervated than the proximal parts and the trunk" (Johansson & Vallbo, 1979).

Several different measurements are used to characterize the skin's spatial acuity: two-point thresholds, grating orientation, relative point localization, and absolute point localization. A two-point threshold is a measure of the minimum distance between two points required for a person to be able to distinguish them as being separate. This is often measured using gap detection, which measures the minimum gap length required for subjects to distinguish between a broken or unbroken line of equal length (Stevens & Choo, 1996). Two-point thresholds are positively correlated with receptor field size, that is the smaller the receptor field size the smaller the two-point threshold. Grating orientation measures subjects' ability to identify the alignment of a straight edge on the skin (Gibson & Craig, 2005). Relative point localization refers to the minimum distance required for subjects to determine the orientation of a second point with reference to the first. Absolute point localization is a measure of how accurately a person is able to locate a single point of stimulation on the skin. All three of these measurements aim at characterizing spatial acuity but are based on different procedures and thus produce different thresholds at a given body site. Values for each of these thresholds also vary noticeably across the body. Some variation in acuity between individuals can be attributed to the effects of age and gender (Cholewiak et al., 2001; Gescheider et al., 1994; Stevens & Choo, 1996).

Many researchers have tried to define average values for these thresholds of spatial tactile acuity, yet there is still some variation between results. Table 1 shows two-point gap thresholds, and relative point localization values.

	2-point gap thresholds (mm) in proximal-distal direction [1]	2-point gap thresholds (mm) proximal-distal; medial-lateral, and (ratio) [2]	Relative point localization (mm) [1]
Finger tips	1.1	1.08 ; 1.61 (0.67:1)	
Finger base	3.5	5.13 ; 3.62 (1.42:1)	
Palm	6.3	7.17 ; 5.30 (1.35:1)	2.3
Forearm, ventral	17	22.93 ; 9.75 (2.35:1)	7.3
Upper arm, lateral	21	20.07 ; 12.21 (1.64:1)	
Thigh, ventral	16		
Foot sole, center	10		2.7
Big toe (hallux)	4.0		1.4

Table 1. Values for two-point gap thresholds and relative point localizations for people aged 20 to 25. [1](Stevens & Choo, 1996), [2](Gibson & Craig, 2005)

The data from Gibson and Craig (2005) in Table 1 show a sensitivity anisotropy (directional dependency) along the skin, where for most sites the sensitivity is significantly greater in the medial-lateral direction (across the limbs) than in the proximal-distal direction (along the length of the limbs). On the fingertips this anisotropy is reverse with greater sensitivity in the proximal-distal direction, which is attributed to the orientation of the gap contactor relative to the skin ridges. The sensitivity is higher when the gap edge is oriented perpendicular to the dermal ridges as opposed to parallel (Gibson & Craig, 2005).

Although specific values for two-point thresholds, relative point localization, and absolute point localization depend on the measurement protocol, consistent trends in tactile sensitivity have been reported. Several researchers have found consistent trends that tactile sensitivity increases with distance from the trunk in a proximal to distal direction on the limbs, which is consistent with the density of innervation (Gibson & Craig, 2005; Stevens & Choo, 1996).

2.2 Sensitivity to Vibration

Human sensitivity to vibration falls within the range of frequencies from 0.4 Hz to greater than 500 Hz depending on the amplitude of vibration (Bolanowski et al., 1988). Vibration is primarily sensed by the rapidly adapting receptors, although the slowly adapting receptors also sense certain frequency ranges. Merkel disk receptors, which are slowly adapting mechanoreceptors (SA I), are the most sensitive to very low frequency vibrations in the range of 0.4-3 Hz, which tend to produce sensations of

pressure (Bolanowski et al., 1994). The other slowly adapting receptor (SA II), the Ruffini end organ, is relatively insensitive to vibrations but can sense frequencies in the range of 100-500< Hz, in which a buzzing sensation has been reported (Bolanowski et al., 1994). The rapidly adapting (RA I) Meissner's corpuscles in glabrous skin sense low frequencies in the range of 3-40 Hz (Bolanowski et al., 1994), which is often perceived as "flutter." Lastly, the Pacinian corpuscles, a rapidly adapting type 2 receptor (RA II), are most responsible for the sensation of vibration, sensing frequencies in the range of 40-500< Hz (Bolanowski et al., 1994). Although both rapidly adapting receptors are sensitive to vibrations, the Meissner corpuscles require much larger amplitudes than the Pacinian corpuscles which can sense vibrations with amplitudes as low as 1 μm at 250 Hz (Gardner et al., 2000). Humans are most sensitive to frequencies in the range of 200-250 Hz (Konietzny & Hensel, 1977). Frequencies outside of this range must have proportionally greater amplitudes to be felt. Tuning curves are often used to display this relation between minimum vibration amplitude and frequency that defines the thresholds of detection for both receptor activation and human perception. Perceptual tuning curves do not follow a constant slope due to activation of different receptors with varying frequency. Each type of receptor has a unique tuning curve, the combination of which determines the perceptual thresholds (Bolanowski et al., 1988; Gescheider et al., 1994). For example, human vibration thresholds measured on the back of the hand decrease rapidly above 40 Hz, at which point subjects report a notable improvement in detecting sensation, with frequencies below 40 Hz feeling like a flutter, whereas frequencies above 60 Hz were felt as vibration (Konietzny & Hensel, 1977). Vibration thresholds on the hairy skin of the hand tested from 10-100 Hz was found to range from about 88 μm (± 26 μm) at 10 Hz to about 6 μm (±8 μm) at 100 Hz (Konietzny & Hensel, 1977).

Threshold differences exist between receptor activation and human perception, because human perception is limited by receptor activation thus perceptual thresholds are always greater than or equal to neural thresholds. Threshold values can also vary with body location, due to variations in innervation density. When comparing threshold values over the frequency range of 8-250 Hz on the fingertip, volar forearm, large toe, and heel, a significant effect of location was found; the fingertip had the lowest average threshold values, followed by the big toe, the heel, and lastly the volar forearm which had the highest thresholds (Morioka et al., 2008). These results follow the same ranking of body part sensitivity as found with two-point gap thresholds (Gibson & Craig, 2005; Stevens & Choo, 1996), and again demonstrates the improved sensing ability of glabrous as compared to hairy skin.

Several factors have been found to effect vibration thresholds, including the size of the contact area and skin temperature. Larger stimuli or larger contact areas were found to produce significantly smaller threshold values signifying higher sensitivity (Bolanowski et al., 1994; Gescheider et al., 1994; Morioka et al., 2008). Skin temperature was also found to significantly affect sensitivity to vibration, with warmer skin temperature tending to lower the amplitude threshold, and cold increasing it (Bolanowski et al., 1994). This is especially evident at mid to high-frequencies (4-300 Hz).

2.3 Physical Skin Properties and Response to Mechanical Perturbation

Several different techniques have been used to try to characterize the skin's response to a dynamic mechanical perturbation or indentation. Boyer et al. (2007) quantified the viscoelastic properties of human skin in vivo with the use of dynamic indentation. They used a probe to apply a small sinusoidal indentation ranging from 10-60 Hz to the surface of the forearm while simultaneously measuring the resulting force and displacement of the probe on the skin. Results of this study found the mechanical behavior of skin in response to a dynamic indentation followed a Kelvin Voigt model, in which physical properties such as stiffness and damping are independent of frequency. This study also showed that although the skin's physical properties remained constant regardless of frequency, they also varied greatly based on skin location, varying in stiffness by as much as 110% over a 120 mm section of forearm.

Two studies involving optical coherence tomography (OCT) and optical coherence elastography (OCE) techniques also found that the elastic properties of skin varied with body location (Li et al., 2011; Liang & Boppart, 2010). Using these techniques they calculated the Young's moduli of the skin on the palm and forearm based on surface wave phase-velocity relations. By varying the frequency of applied of vibration, Liang and Boppart (2010) theorized that they could determine the properties of different skin layers. They took measurements orthogonally to the skin's Langer's lines during an applied 50 Hz driving frequency, and reported that the average Young's modulus of the stratum corneum was larger for the volar (101.18 kPa) and dorsal (68.68 kPa) forearm than the palm (24.91 kPa). Another study by Li et al. (2012) which measured the skin at a much higher applied frequency of 1-5 kHz in a direction parallel to Langer's lines found the Young's modulus was higher for the palm (254.57 kPa) than the forearm (202.0 kPa). Both studies found a variation in Young's modulus as the applied frequency increased, which they attributed to the influence of different skin layers with varying stiffness. Liang and Boppart's (2010) results at 600 Hz also indicated anisotropic skin stiffness behavior, where the skin

stiffness was found to be much greater in the direction parallel to the skin's Langer lines as compared to the orthogonal direction. However, at a lower driving frequency of 50 Hz the stiffness in both directions was comparable, producing no obvious anisotropy.

A few studies have looked into the transmission of physical waves on skin. An early study by Franke et al. (1951) on the thigh (over the rectus femoris), found that the amplitude of surface waves created by a sinusoidally vibrating piston oriented perpendicularly to the skin decreased in inverse proportion to the travel distance squared ($1/d^2$). A study on a skin-like substrate called Skinsim found that the amplitude attenuation of mechanical vibrations fit a Gaussian distribution curve (Jones & Held, Characterization of tactors used in vibrotactile displays, 2008).

2.4 Tactile Displays

2.4.1 Types and Uses for Tactile Displays

There are a variety of tactile displays that range in function and type of stimuli delivered to the skin. Some displays provide tactile feedback in situations where tactile information is lacking, such as in virtual environments where the objective is to make the experience within these environments feel more realistic (Guinan et al., 2012). Tactile displays can also be used as sensory substitution devices, to help people compensate for their impaired sensory system. For example, people with balance impairments caused by damage to their inner ear's vestibular system, can benefit from wearing a vibrotactile array around their waist that uses vibration to alert the wearer to excessive body tilt which may cause them to lose their balance or fall (Wall & Weinberg, 2003). Tactile displays can be used by people with hearing impairments to communicate localized sounds by translating recorded audio signals into electrotactile or vibrotactile pulses of varying intensity and rhythm (Saunders, 1973). Some tactile displays have been used as visual aids to help the visually impaired navigate through their surroundings by providing spatial tactile cues about their immediate environment. These types of tactile displays are also used for other applications, such as providing spatial orientation and navigational cues to pilots (van Erp, 2007).

The key considerations in designing any tactile display are where on the body the display will be mounted and the actuator technology used to present tactile cues. When designing a display for navigation other factors must also be considered, such as ensuring that its placement on the body does not interfere with an individual's ability to move or perform other functions (van Erp, 2007). For

example although the hands have high tactile sensitivity, which is ideal for communicating tactile signals, in many situations the hands must be free to use for other activities. Ideally the tactile signals should evoke an intuitive or reflex-like reaction, so that little training or mental capacity is required to interpret the stimuli (van Erp, 2007). Lastly, as for any portable wearable device, the display must be comfortable, lightweight, unobtrusive physically and visually, and easy to wear.

Not only do tactile displays serve different purposes, but they also use different types of stimuli and actuators: electrical and mechanical. Electro-tactile or electrocutaneous stimulation stimulates the skin by passing electrical pulses through electrodes in contact with the skin (Saunders, 1973). However, electrical stimulation is somewhat unstable and can potentially hurt or injure the user (van Erp, 2007). Mechanical stimuli can be delivered by three main types of actuators: pneumatic, DC-motor based, and coil based. Pneumatic actuators use a combination of pressurized air and valves to mechanically move a membrane that applies pressure to the skin. However, this technology is not ideal for portable tactile displays due to its need for pressurized air (van Erp, 2007). DC-motors produce vibrotactile stimuli by means of an eccentric mass that rotates about a center axis. This type of actuator is commonly used for tactile displays due to its simplicity, but is limited by the fact that it has coupled frequency and amplitude and that it does not vibrate along a single axis, but rather produces a more multi-dimensional vibration. Coil-based actuators provide vibration along a single axis, and allow independent control of vibrational frequency and amplitude (van Erp, 2007). All of these actuator types can produce signals that vary in intensity and frequency. In the research described in this thesis, DC-motors were used.

2.4.2 Tactile Displays for Spatial Cuing

Accurate localization of tactile stimuli is important when displays are used to communicate spatial cues for guidance and navigation. Several factors have been found to affect localization accuracy in vibrotactile displays including the site of placement of the array on the body, the locations of the motors with respect to specific anatomical landmarks, variations in stimulus frequency, and the number and spacing of motors in the display.

The key factor in determining the effectiveness of tactile displays for spatial cuing, given a specific body placement, is the number and spacing of motors. When designing vibrotactile displays the spacing between motors cannot be determined solely by two point threshold values since these are based on static as opposed to dynamic stimuli. When using multiple vibrating motors designers must expect that the vibrotactile signal will spread beyond the limits of the contactor area resulting in signal interference

between motors (Cholewiak et al., 2001). When a three-by-three array of motors with 25 mm inter-motor spacing was placed on the forearm above the wrist and activated at 150 Hz, subjects were asked to identify the location of individual motors as they were activated. The results of this absolute identification test showed that the location of only five out of the nine motors could be identified with more than 50% accuracy, and that the location of only two motors could be absolutely identified as defined by information transfer values (Chen et al., 2008). Results of this test revealed that subjects were more able to identify the position of a motor along the medial-lateral axis (across the limb) as opposed to the proximal-distal axis (along the length of the limb), as indicated by the better identification of the activated column as opposed to the activated row. Higher resolution along the medial-lateral axis as opposed to proximal-distal was also found when subjects were asked to identify moving vibrotactile patterns presented on a three-by-three array mounted on the volar forearm (Jones et al., 2009).

Several studies have shown that certain "anchor point" locations of a tactile display are more easily recognized than other locations (Cholewiak et al., 2001; Salzer et al., 2010). On the thigh, Salzer et al. (2010) used a band of eight equally spaced motors strapped around the leg that stimulated the skin at 250 Hz. They found that the motors located in the center frontal and center dorsal (rear) positions were located with the highest accuracy, and the direct lateral and medial positions had the lowest identification accuracy. Salzer et al. (2010) also found that the accuracy on the thigh increased significantly as the tactor band was placed closer to the knee and further from the groin. Spatial localization accuracy has also been tested using a belt around the lower abdomen containing twelve equally spaced motors vibrating at 250 Hz at 150 msec bursts (Cholewiak et al., 2001). This experiment also showed evidence of optimal identification accuracy at anchor points located at the navel (center frontal) and spine (center dorsal) (Cholewiak et al., 2001).

Experiments conducted on the forearm by Cholewiak and Collins (2003) tested the absolute localization identification of seven motors located linearly along the forearm driven in 500 msec bursts at 100 Hz or 250 Hz. They found that the two motors at either end of the array (closest to the elbow and wrist) had the highest identification accuracy: 72% and 74% correct at 100 Hz and 250 Hz respectively compared to 40% for the center motors. When the linear array was moved proximally up the arm so that it crossed the elbow (where motor 4 was at the elbow, motor 1 was the most distal on the volar forearm and motor 7 was most proximal on the upper arm), the highest localization accuracy occurred at the elbow, with roughly 83% accuracy. When comparing the localization accuracy of the

two end points to previous results, they found that the accuracy of the most distal motor, now located in the middle of the forearm, significantly decreased from around 74% to 42% correct localization, going from the highest to lowest relative localization accuracy, and that the most proximal motor maintained the same accuracy (69-71%) (Cholewiak & Collins, 2003). When looking at the identification accuracy as a function of absolute location on the arm as opposed to location within the array, accuracy only varied by about 5-10% (Cholewiak & Collins, 2003). Information transfer revealed that proximal movement of the array so that it crossed the elbow increased the average number of locations that could be accurately identified from 2.48 locations (1.28 bits) to 3.18 locations (1.67 bits) out of a possible 7 locations (2.81 bits). This suggests that "anchor points" may be determined primarily by relative proximity to anatomical landmarks as opposed to their relative placement within an array configuration. Cholewiak and Collins (2003) also found that the higher accuracy "landmark" effect could be artificially recreated by changing the frequency of a single motor within an array (100 Hz versus 250 Hz and vice versa).

Other work by Cholewiak and colleagues has looked into the effects of stimulus frequency on localization accuracy, and found that uniform variations in frequency from 100 Hz and 250 Hz had little effect on localization accuracy on the forearm (Cholewiak & Collins, 2003; Cholewiak et al. 2001). Although a consistent frequency change across all stimuli did not have a significant effect on localization accuracy, varying the frequency of a single motor did have a significant effect on localization accuracy, improving the accuracy for the unique motor (Cholewiak & Collins, 2003). Localization accuracy was also found to be independent of vibration thresholds given that a nearly uniform threshold was measured along the length of the forearm (Cholewiak & Collins, 2003).

Some studies have found that increasing the spacing between motors has a positive impact on localization accuracy (Cholewiak & Collins, 2003; Cholewiak et al. 2001). Cholewiak et al. (2001) found that by reducing the number of motors from seven to four and doubling the inter-motor spacing from 25 mm to 50 mm along the forearm the accuracy increased from 40%-75% to 70%-90% correct. A similar experiment, in which the spacing of the seven motors was increased from 25 mm to 50 mm along the length of the arm from the wrist to the shoulder (Cholewiak & Collins, 2003), showed an overall increase in accuracy from 55% to about 80%, improving from roughly 33%-77% correct to 65%-90%. Given these results, Cholewiak and Collins (2003) hypothesized that this may indicate that the threshold distance for localization of vibrating stimuli on the forearm is greater than 50 mm.

2.5 Research Objectives

The objective of the current study was to see if the characteristics of surface waves induced by vibrotactile stimulation differed significantly at three locations on the body: the palm of the hand, the volar surface of the forearm, and the anterior surface of the thigh. These locations are often considered when tactile displays are used for spatial cuing. An array of accelerometers was used to measure the frequency and amplitude of the surface waves on the skin and to determine how far the surface waves travelled and how quickly they attenuated. Results from this research would give insight into how far apart motors should be spaced on different parts of the body in order to avoid signal interference by traveling waves. Part of the results from this work has been published (Jones & Sofia, 2012).

Physical measurements provide the basis for understanding the impacts to sensory systems. The second part of this research studied the somatosensory system's ability to localize vibrations. Psychophysical experiments were performed using a three-by-three array of motors to determine subjects' ability to accurately locate the source of perceived vibrations at the same three body locations (palm, forearm, and thigh), and to see how this absolute localization accuracy varied as a function of body location and inter-motor spacing. From these experiments we hope to gain information about the inter-motor spacing distances required for accurate spatial cuing, and whether this varies at different sites on the body. Both the physical and psychophysical experiments should provide valuable information on how to configure motors in a vibrotactile display used to communicate spatial cues.

3. Preliminary Tactor Characterization Experiments

Sanko Electric (Model 1E110) pancake motors were used in all the experiments. These motors are 14 mm in diameter and 3.5 mm thick. They vibrate when activated due to an eccentric mass which rotates around the center of the motor. When the motor is placed on the skin, the rotation occurs in the plane parallel to the skin surface. Before these motors could be used in human experiments the motors' performance had to be characterized to determine the expected frequency and amplitudes of vibration at specific input voltages. Analyses of high speed video recordings and measurements made when the motors were mounted on an impedance head were used to characterize the motors.

3.1 High Speed Video of Tactor Vibrations on Skin

High speed video recordings where used as one initial test method to acquire reference measurements of the motors' performance on skin. The high speed video recordings were taken of a pancake motor vibrating while mounted on a human forearm. These videos were then analyzed to find approximate vibrational frequency and amplitude values to use as a reference to ensure viable accelerometer measurements.

3.1.1 Methods

High speed video recordings where taken using the Phantom V9.0 high-speed camera (Vision Research) at a sampling rate of 500 frames per second. Video recordings were taken of the pancake motor vibrating while mounted on the forearm. The motor was attached to the skin with double sided tape, and was powered at 2, 3 and 4 volts. The video recordings were then analyzed using Phantom software, by first scaling the video and then tracking the coordinates of a single point at the intersection of the motor and the skin.

3.1.2 Results

The results of the high speed video testing showed that the average vibrational motor frequency for two motors run at 2, 3, and 4 volts on the forearm was about 30, 35, and 41 Hz respectively. The average amplitudes at these three voltages were about 0.58, 0.69, and 0.86 mm in the horizontal plane parallel to the skin, and about 0.27, 0.36, and 0.44 mm in the vertical direction normal to the skin surface. Due to limitations in human ability to distinguish the available video resolution, the recorded

amplitudes are expected to be less accurate than the recorded frequencies. Some variability in frequency is likely to occur between motors as well as for a single motor, which can vary in frequency by as much as 12 Hz (Jones & Held, Characterization of tactors used in vibrotactile displays, 2008). Figure 1 below shows a plot of the vibrational amplitude in both directions as acquired from the high speed videos.

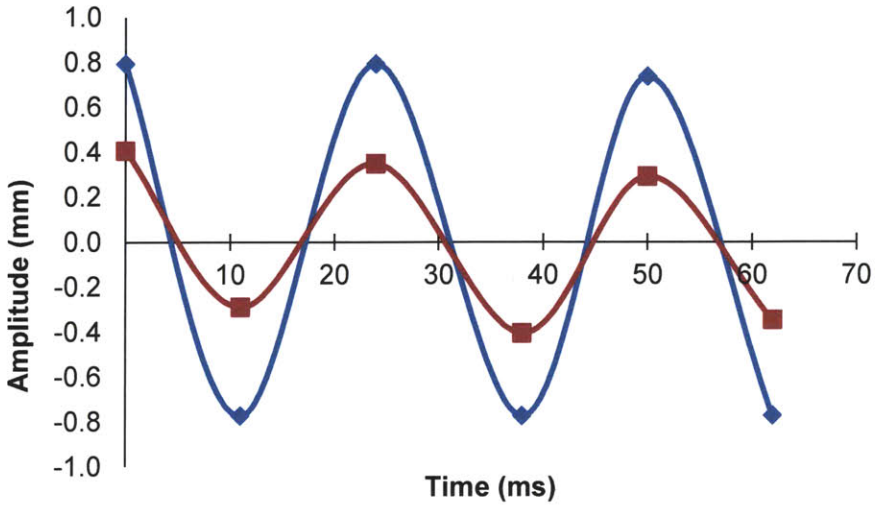

Figure 1. A plot of the sinusoidal motion of a pancake motor on the forearm as it vibrates at 41 Hz with a supply voltage of 4 Volts. The blue line illustrates the movement in the horizontal plane and the red line illustrates the vertical movement occurring normal to the skin surface.

3.2 Measuring Tactor Frequency with Impedance Head

A second method of motor characterization was performed using a Brüel and Kjaer impedance head (Type 8001) and charge amplifier (Type 2635). By first characterizing each motor's frequency as a function of input voltage when mounted on a rigid structure, these data could then be used to determine how much the frequency changed when the motor was mounted on a more compliant surface such as the skin.

3.2.1 Methods

To characterize motor performance, each motor was glued to a threaded pin and mounted on its side to the impedance head which was connected to a charge amplifier. Once the motor was properly mounted, it was powered by a DC power supply (Agilent E3632A) at specified voltages (2 V, 3 V, and 4 V). Each motor was tested 10 times, with each trial lasting 4-5 seconds. Through the use of a

piezoelectric accelerometer and force gauge, the impedance head sensed the force and velocity of vibration at a single point. This mechanical signal was then converted to an electric charge through transducers within the impedance head. The charge signal from the impedance head then passed through the charge amplifier for filtering and amplification, through a data acquisition system (National Instruments USB-6251), and into the computer for processing in LabVIEW. A LabVIEW program used a Fast Fourier Transform (FFT) and a Harmonic Distortion Analyzer to identify each motor's frequency of vibration.

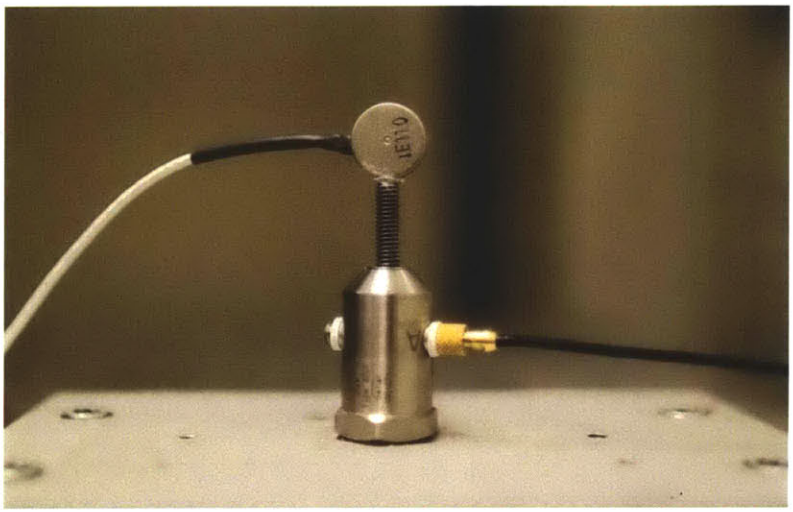

Figure 2. Pancake motor mounted on the impedance head. Test setup used to characterize motor frequency.

3.2.2 Results

The results of the impedance head measurements showed that the average frequency of vibration of ten motors was 62.7 Hz, 94.0 Hz, and 113.2 Hz when powered at 2, 3, and 4 V respectively, with corresponding standard deviations (SD) of 10.9 Hz, 22.0 Hz, and 24.9 Hz. For motor number 4, which was used for skin measurements the average frequency measured was 52.9 Hz (SD: 2.1), 72.6 Hz (SD: 2.4), and 88.4 Hz (SD: 2.6) at 2, 3, and 4 V respectively. Motor number 8, which was used for the bi-directional skin measurements, had higher average frequencies of 63.6 Hz (SD: 4.5), 93.0 Hz (SD: 0.6), and 119.6 Hz (SD: 2.7) at 2, 3, and 4 V respectively. The means of the data from all ten motors show that the mean frequency increases by an average of 25 Hz per volt, following a linear trend of $f = 25.3x + 14.1$, where f is the average frequency and x is the supply voltage.

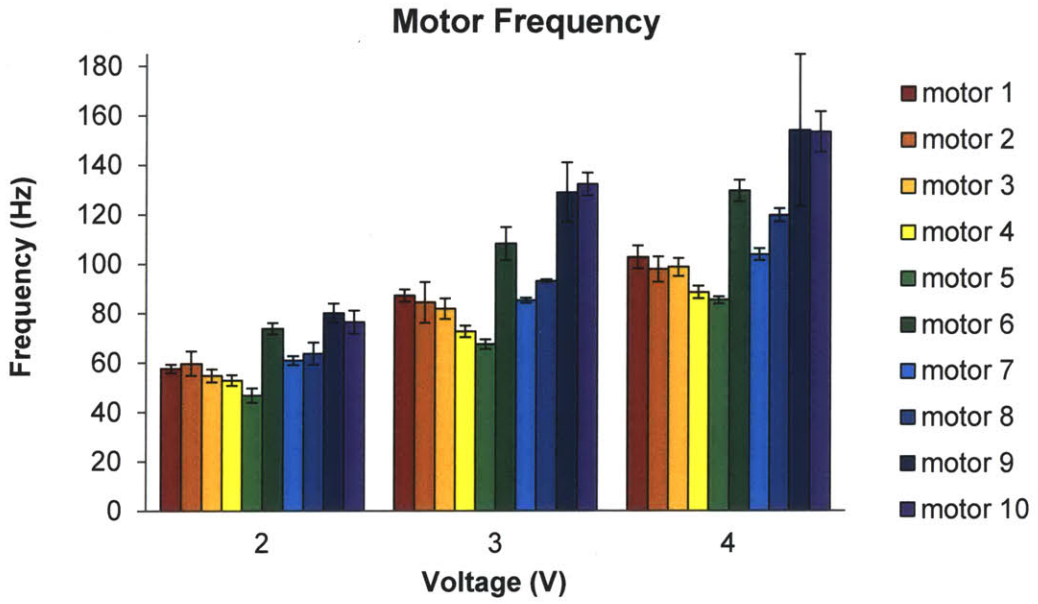

Figure 3. Mean frequency measurements of ten pancake motors tested at 2, 3, and 4 V on the impedance head

Overall the results of these impedance head measurements showed that there is considerable variability in frequency between motors, which ranged from 67.4 Hz to 131.9 Hz at 3V. The frequency of a single motor also varied from trial to trial. The standard deviation of the individual motor frequency varied from 0.6 to 12.0 Hz at 3 V with an average standard deviation of 4.4 Hz. These results agree with previous tactor characterization experiments performed on the same type of motors (Jones & Held, Characterization of tactors used in vibrotactile displays, 2008), which also found that the average frequency of vibration varied across motors, ranging from 92.9 Hz to 162 Hz at 3.3 V with an average of 134.9 Hz (SD: 20.8 Hz). They also found that most motors varied in frequency by an average of 6.8 Hz (1.2 to 12 Hz), with the exclusion of one highly variable motor, whereas our motors were slightly more variable and varied by an average of 12.7 Hz at 3 V.

4. Measuring Vibration on Skin with Accelerometer Array

Since the amplitude of vibration influences the ability to perceive the frequency of vibration, it is of interest to measure the frequency and amplitude of the vibrotactile stimulus provided by a vibrating motor on the skin, as well as the resulting surface wave amplitude as it travels along the skin. Measurements were taken at three sites on the body commonly used for tactile input—the palm, forearm, and thigh—with the objective of determining whether varying skin properties affected the frequency and amplitude with which the motor vibrated and how to measure the surface waves attenuated as they moved along the skin. These measurements would also provide useful information to help determine the spacing between tactors in a vibrotactile display used for spatial localization.

The initial intent was to design an accelerometer array capable of simultaneously measuring the surface wave at multiple points on the skin. Due to the multi-dimensional vibrational movement elicited by the selected motors, as opposed to a more one-dimensional localized movement characteristic of other tactors, it made sense to measure the vibration in all three axes of acceleration. The accelerometer array was initially designed with eight accelerometers: two accelerometers to measure the motor vibrations, one for each of the two motors, and six other accelerometers distributed around and between the motors to measure the surface waves on the skin in different directions and distances. The spacing between the accelerometers was chosen such that it would capture the extent of the traveling wave on the skin (Jones et al., 2010).

Two different experiments were done the accelerometer arrays. In the first experiment, the surface waves induced by vibration were measured in one direction along the skin at each site. In the second experiment, the surface waves were measured in both the proximal-distal (longitudinal) and medial-lateral (transverse) directions at all three body sites.

4.1 Design and Fabrication of Accelerometer Array

A flexible printed circuit board (PCB) containing eight 3-axis micro-accelerometers (StMicro LIS331DLH) was designed and fabricated for experimental measurements. The PCB layout was designed using Eagle (Version 5.11.0 Standard Edition). A picture of the circuit design and the board layout are shown in Figures 4-7. The flex PCB fabricated by Sunstone Circuits was constructed out of layers of kapton and adhesive containing two trace layers of 1 ounce copper wiring, resulting in a total thickness of about 0.2 mm. Board population was performed by Flex Interconnect Technologies. Each PCB array

contains eight 3-axis micro-accelerometers with a sensing range of up to ±8 g and requires 2.5 V input voltage. Each PCB also contains eight 10 µF tantalum capacitors (AVX Corporation TLCK106M006QTA), eight 0.1 µF ceramic capacitors (Yageo (VA) CC0603ZRY5V7BB104), and one voltage regulator (National Semiconductor LP2985AIM5-3.3/NOPB) to reduce the input voltage from 5 V to 2.5 V. A full list of circuit components is provided in Appendix 1. PCB Components and Construction Specs

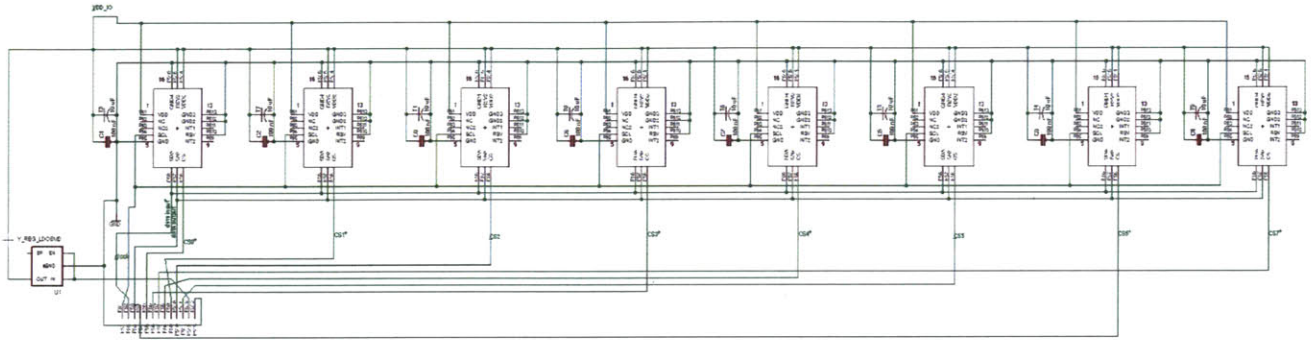

Figure 4. Circuit schematic from Eagle of accelerometer array for printed circuit board.

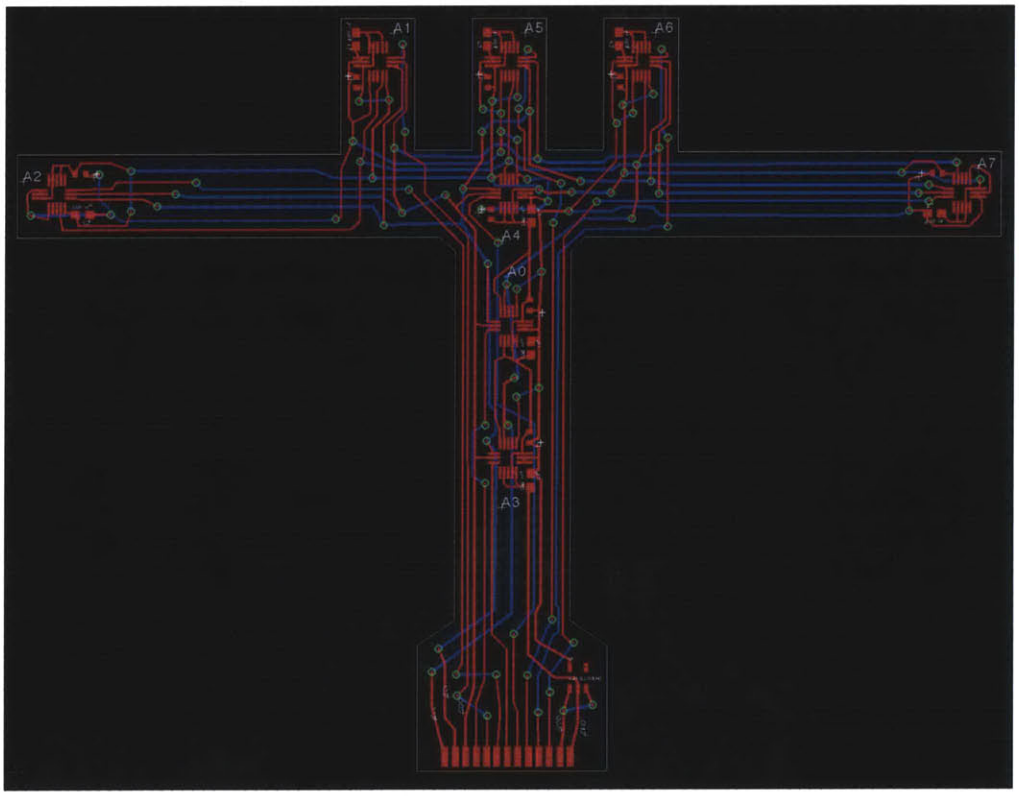

Figure 5. Screen capture of the final printed circuit board layout in Eagle showing both layers: top (red) and bottom (blue).

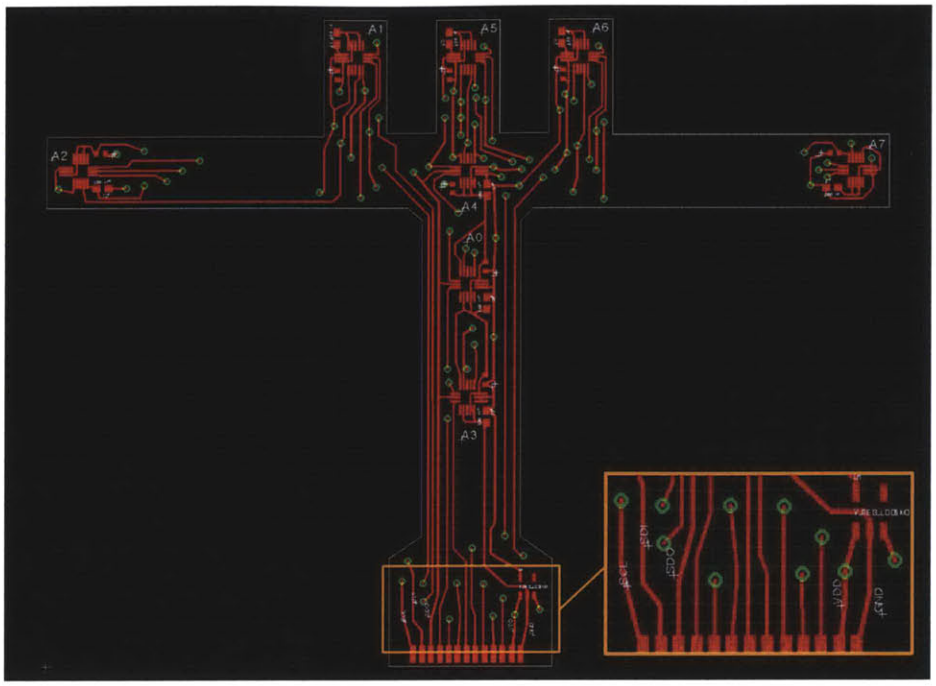

Figure 6. Top layer of PCB layout from Eagle. Wire traces and contact pads are shown in red, vias a.k.a. connection holes are shown as green circles, and the silk screen labels are shown in white. The location of each accelerometer is marked by an accelerometer number (A#) label next to the designated pads. The numbering indicates the order in which the chip select lines fall along the bottom connection pads.

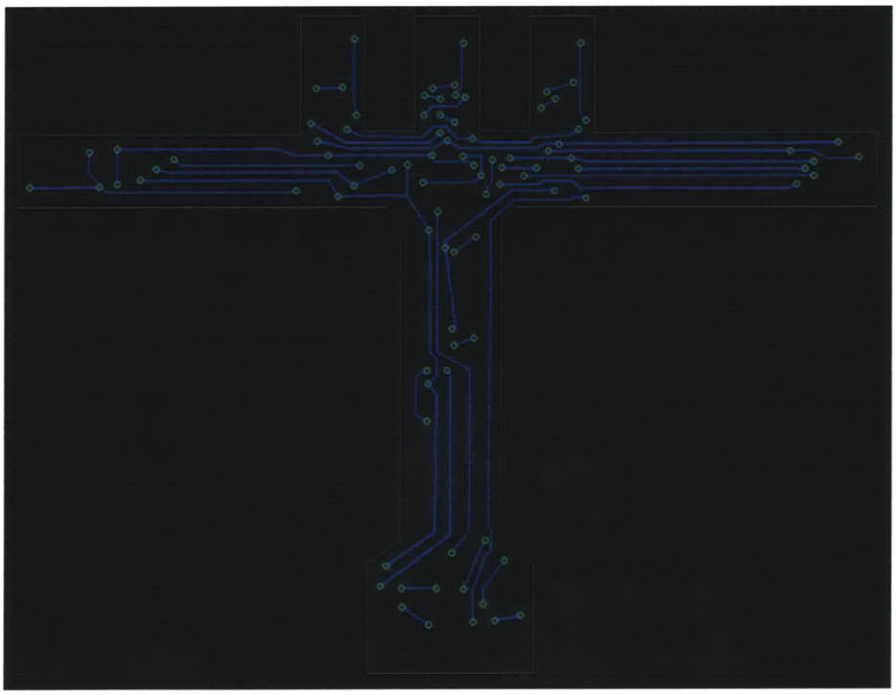

Figure 7. Bottom layer of PCB layout from Eagle. Wire traces are shown in blue and vias a.k.a. connection holes are shown as green circles.

The initial intent of this design was to use only one array to take measurements, collecting data from all eight accelerometers simultaneously. The long side strips of the PCB were designed so that they would bend when attached to motors on the skin. The spacing between accelerometers, with the exception of A2 and A7 (as shown in Figures 5 and 6) on the far side arms is 16 mm. Figures 8 and 9 show pictures of the final populated flex PCB.

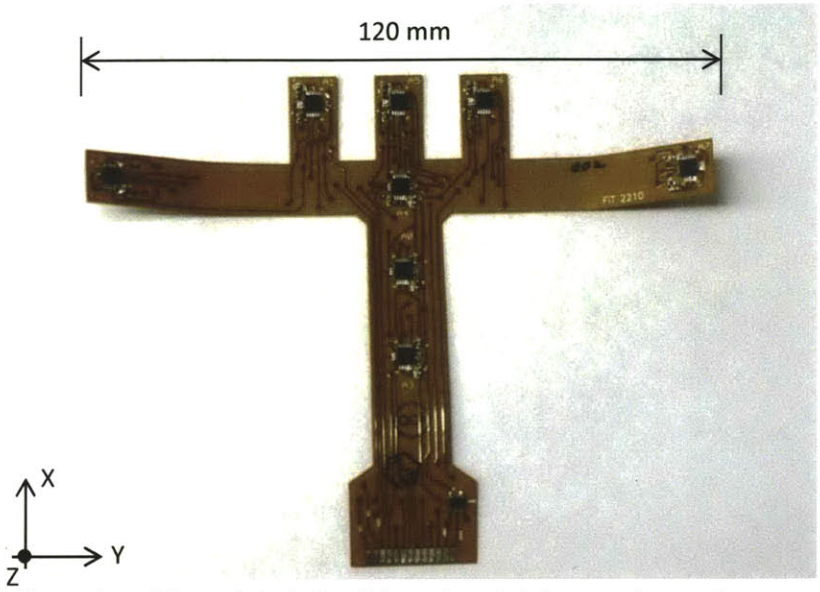

Figure 8. Unwired populated flex printed circuit board containing accelerometer array. The X-Y axis shows the orientation of the axes of acceleration as detected by the accelerometers, where the Z-axis lays normal to the X-Y plane.

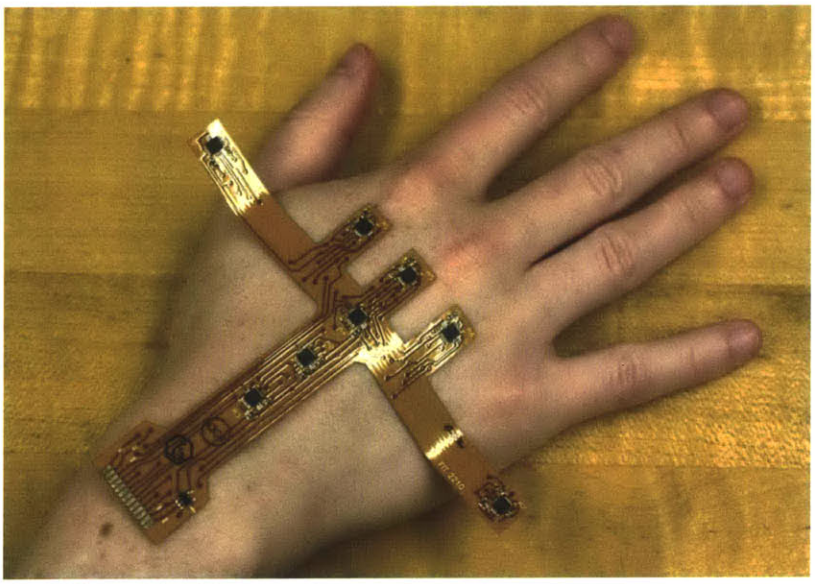

Figure 9. A populated flex printed circuit board placed on a hand. The array shown does not have wires connected.

4.2 Uni-directional experiments

4.2.1 Experimental Methods

Eight subjects were tested, four males and four females, ranging in age from 22 to 26 years old. A pancake motor was first affixed to the subjects' skin with double-sided tape and two PCB accelerometer arrays were also attached with tape, one on top of the motor and one on the skin at a set distance. The initial intent was to use a single accelerometer array to measure the motor and skin vibrations, however to eliminate vibrations that may be transmitted through the flex PCB material two separate arrays were used, one for the motor and one for the skin. Once the motor and arrays were secured in place the motor was connected to an adjustable DC power supply (Agilent E3632A) and vibrated while measurements were taken with the PCB array.

Data were collected from the two accelerometer arrays through a National Instruments NI USB-8451 and into a LabVIEW program, at a bit rate of 10 kHz resulting in a 90 Hz or 180 Hz sample rate per accelerometer axis depending on whether the two accelerometers were sampled simultaneously or consecutively. Most of these tests were measured at a 90 Hz sample rate, with the exception of the palm measurements that approached 45 Hz (the Nyquist frequency), which were taken at 180 Hz sample rate. For all tests only one accelerometer was sampled per array, one on the motor and one on the skin closest to the motor so that nothing touched the skin between the motor and the point of measurement.

This process was repeated on three body locations: the palm of the hand, the volar surface of the forearm, and the inner anterior surface of the thigh. At each body site acceleration measurements were taken on the skin at three distances from the vibrating pancake motor in increments of 8 mm (8 mm, 16 mm and 24 mm). The pancake motor was activated at three different supply voltages: 2 V, 3 V and 4 V. Each measurement lasted ten seconds and was repeated five times.

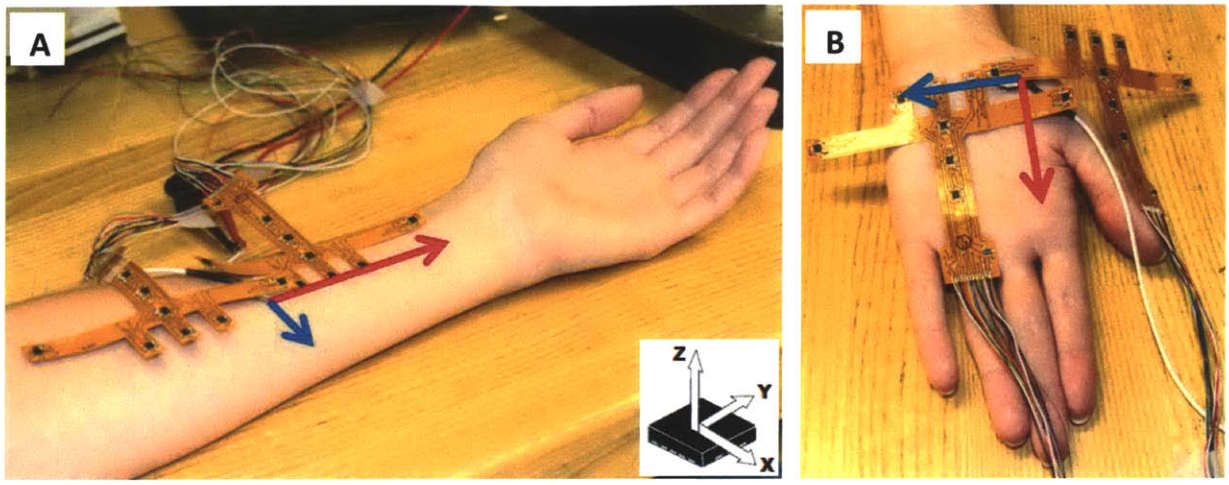

Figure 10. Test setup on the forearm (left) and the palm (right). The arrows indicate the longitudinal (red) and transverse (blue) directions for bi-directional testing. In Figure 10A, the array is setup for testing in the longitudinal direction (along the red arrow), whereas in Figure 10B the palm shows the test configuration for transverse measurements (along the blue arrow). The schematic in the corner of Figure 10A shows the axis orientation only for Figure 10A, however in all cases the Y-axis of acceleration aligns with the straight line between the two active accelerometers.

After the data were read from the accelerometers they were converted in LabVIEW from two's complement into a decimal value for acceleration in units of m/s^2. Vibrational waveforms for each axis of acceleration were collected from the accelerometers and saved as time domain signals. The time signals were then analyzed using a Fast Fourier Transform (FFT) and a harmonic distortion analyzer in LabVIEW to determine each signal's fundamental frequency. The acceleration waveforms were also converted into displacement waveforms, which were then used to find the vibrations' peak amplitude for each axis at each location and supply voltage. Lastly, the collected data were analyzed statistically using IBM SPSS Statistics (Version 20) to determine whether there were significance differences among the measurements as a function of body site and distance. For statistical analyses, the level of significance was set to $\alpha=0.05$ and the p values associated with the F statistics were adjusted using the Greenhouse-Geisser correction.

4.2.2 Results

The results of the initial motor frequency characterization experiments using the impedance head were compared to frequency measurements made on the three body sites to determine where there was a change in frequency when the motors were mounted on the body. These data are shown in Figure 11 where it can be seen that there was a considerable decrease in frequency when the motor was mounted on the more compliant skin surface as opposed to the rigid structure of the impedance head. The frequency was reduced by an average of 50% when mounted on the skin as compared to the impedance head. At 3 V, the overall decrease in frequency averaged 45%, 55%, and 53% for the palm, forearm, and thigh respectively.

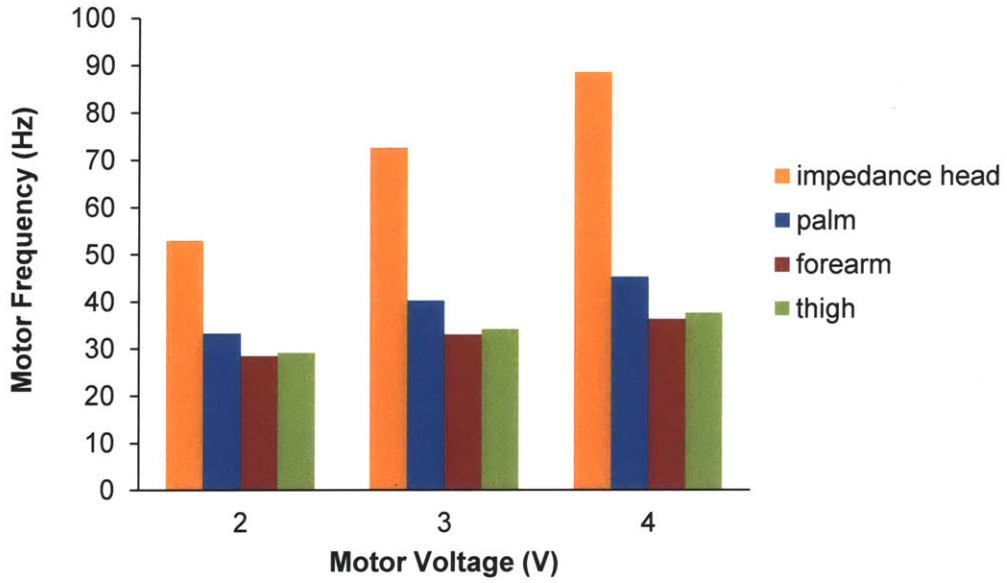

Figure 11. Mean frequency of vibration for a single motor at each location as a function of input voltage.

A comparison of the three body sites tested revealed that the highest frequency of vibration occurred on the palm, reaching 45 Hz at 4 V as compared to 36 Hz and 38 Hz on the forearm and thigh respectively. A repeated measures analysis of variance (ANOVA) with body site and voltage as factors showed a significant effect of body site on the measured frequency ($F(2,14)=18.43$, $p<0.001$), and a significant effect of input voltage ($F(2,14)=272.35$, $p<0.001$). Furthermore, a significant interaction was found between body site and input voltage ($F(4,28)=8.05$, $p<0.01$). The main effect of body site reflects the higher frequencies of vibration measured on the glabrous skin (the palm) as compared to hairy skin. The main effect of voltage indicates that motor frequency increases significantly with input voltage, as expected. The interaction effect presumably reflects the differences in the rate of increase in frequency as a function of voltage at the three sites.

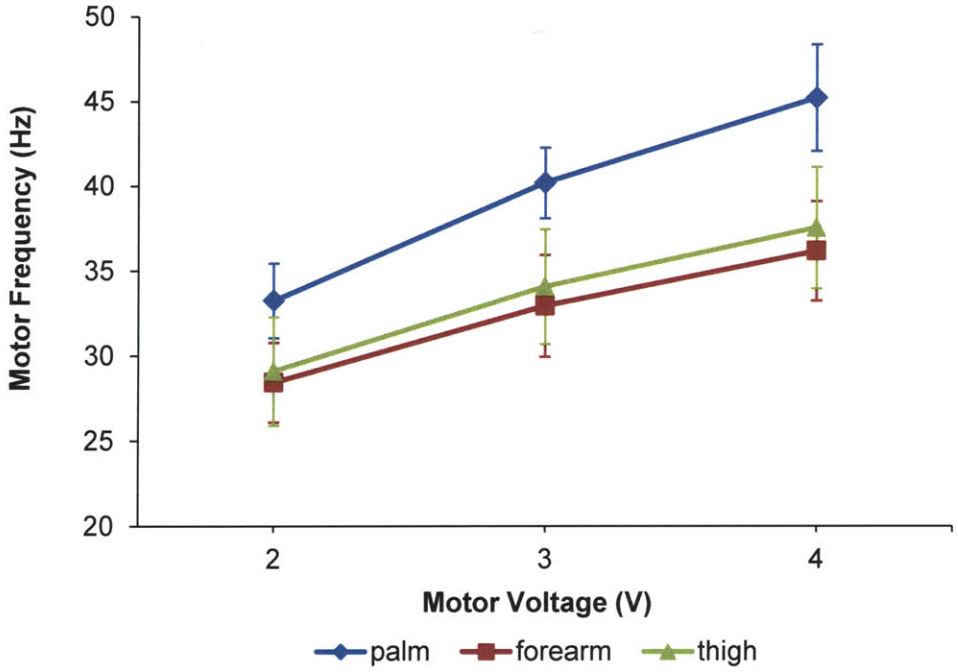

Figure 12. Mean motor frequency measured at each body site as a function of the input voltage. The standard deviations of the means are also shown.

The mean amplitude of the motor oscillation in the Y-axis of acceleration (along the surface of the skin in the line of testing) for each body site and voltage is shown in Figure 13. The figure shows that the palm had the smallest amplitude of vibration, and the thigh the greatest. A repeated measures ANOVA of these data revealed that both body site ($F(2,14)=13.59$, $p<0.01$) and input voltage ($F(2,14)=83.30$, $p<0.001$) were significant, however the interaction was not significant.

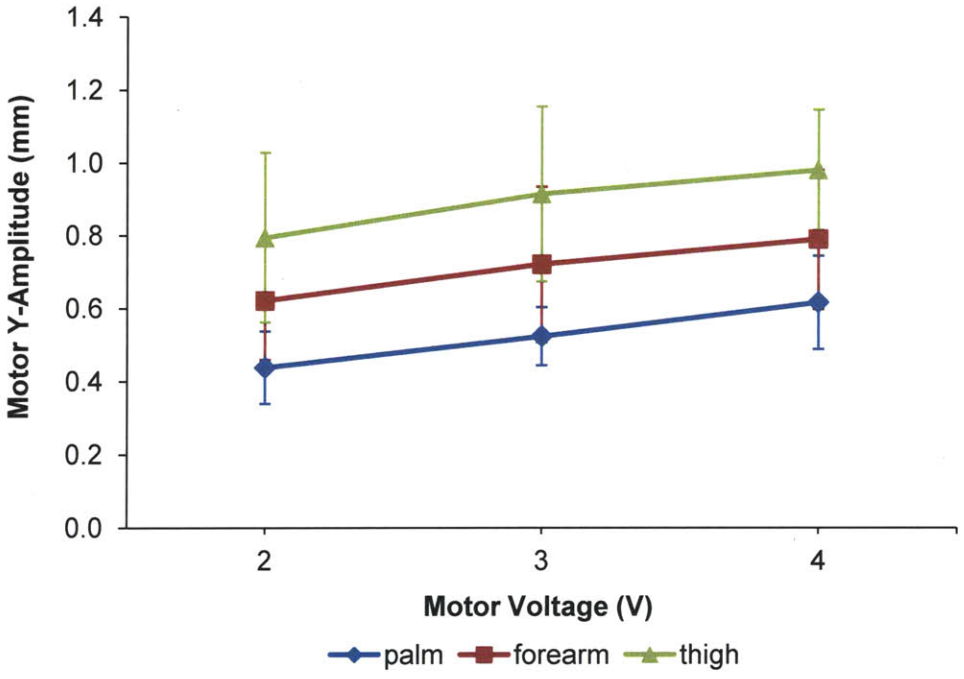

Figure 13. Mean amplitude of motor oscillation in the Y-axis of acceleration (horizontal oscillation) as measured at each body site and at each input voltage. The standard deviations of the means are shown.

Mean amplitudes of the oscillations in the Z-axis of acceleration (normal to the skin surface), are shown in Figure 14. As can be seen in the figure, the amplitudes are very similar for the forearm and thigh and lower for the palm. There was a significant difference in the amplitude measured in the Z-axis of acceleration as a function of body site ($F(2,14)=4.78$, $p<0.05$) and no effect of input voltage.

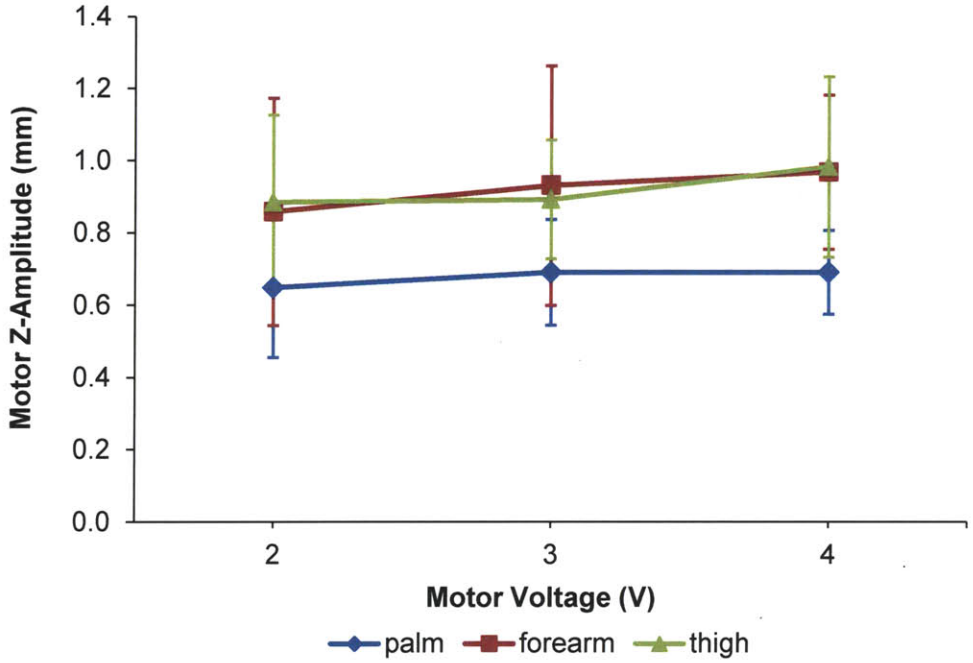

Figure 14. Mean amplitude of motor oscillation in the Z-axis of acceleration (vertical oscillation) as measured at each body site and at each input voltage. The standard deviations of the means are shown.

All three axes of acceleration were measured and converted to displacement to determine the amplitude of vibration. Due to the multidimensional nature of the motors' movements, it made sense to measure all three axes of movement. By measuring all three axes we could also determine the predominant axis of vibration. Figure 15 shows the acceleration measurements for each axis at each distance on the forearm at 3 V. This figure shows that the acceleration occurred predominantly in the X-axis, especially at the motor. However, significant acceleration is also evident along the Y and Z axes. These findings lead to a second experiment in which surface waves were measured in both directions along the skin (Section 4.3).

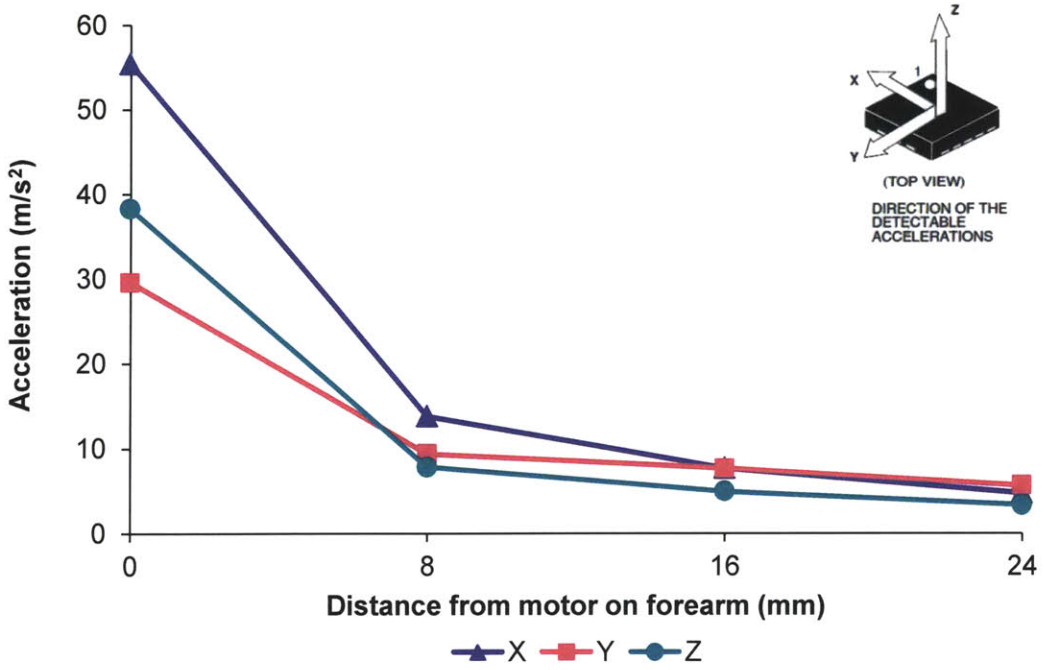

Figure 15. Group mean acceleration on the motor and at 8 mm intervals along the forearm in the three axes of acceleration. Accelerations were predominantly in the X-axis (transverse or across the arm) on the motor, although there was notable motion in both the Y (longitudinal) and Z (normal to the skin) axes.

Plots of the vibration amplitude on the motor (0 mm) and at 8, 16, and 24 mm from the motor are shown for each site in Figures 16-18. Three separate two-way repeated measures ANOVA with distance and body site as factors, revealed that distance (X-axis: $F(3,21)=198.46$, $p<0.001$; Y-axis: $F(3,21)=337.19$, $p<0.001$; Z-axis: $F(3,21)=305.75$, $p<0.001$) was a significant factor for all three axes, and body site (X-axis: $F(2,14)=5.10$, $p<0.05$; Z-axis: $F(2,14)=5.41$, $p<0.05$) was a significant factor for the X and Z axes. Repeated measures ANOVA also revealed that there was a significant interaction between body site and distance (X-axis: $F(6,42)=6.28$, $p<0.05$; Y-axis: $F(6,42)=9.86$, $p<0.005$) for both the X and Y axes. This interaction is most likely due to the notable difference in attenuation in the X and Y axes as well as the distinctly different motor amplitudes in the X and Y axes, whereas the Z-axis for the arm and thigh attenuate at nearly the same rate.

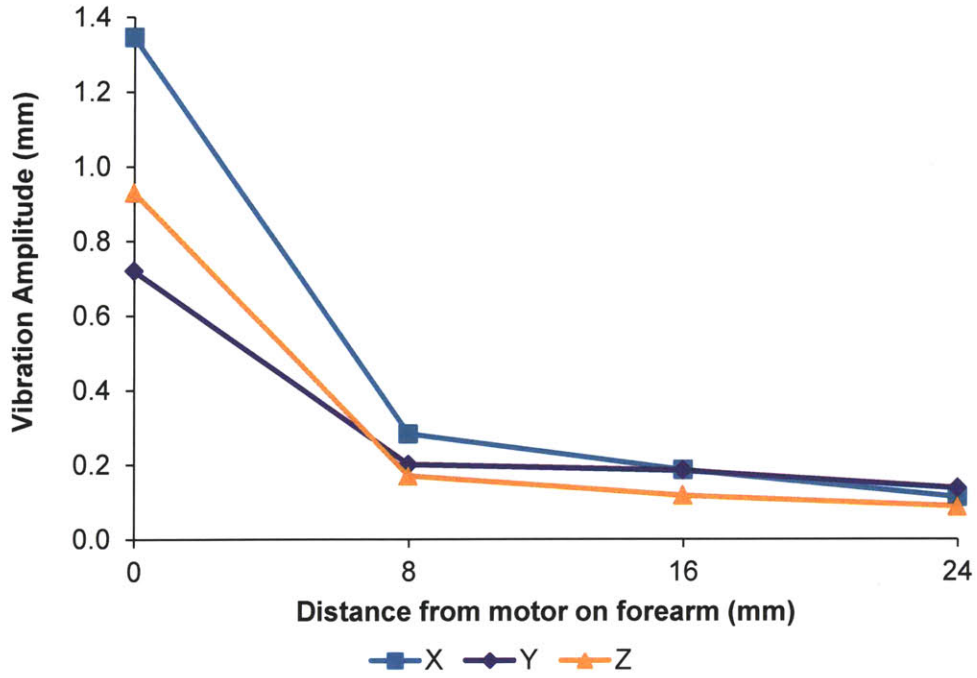

Figure 16. Surface wave amplitude as a function of distance along the forearm in each axis of acceleration.

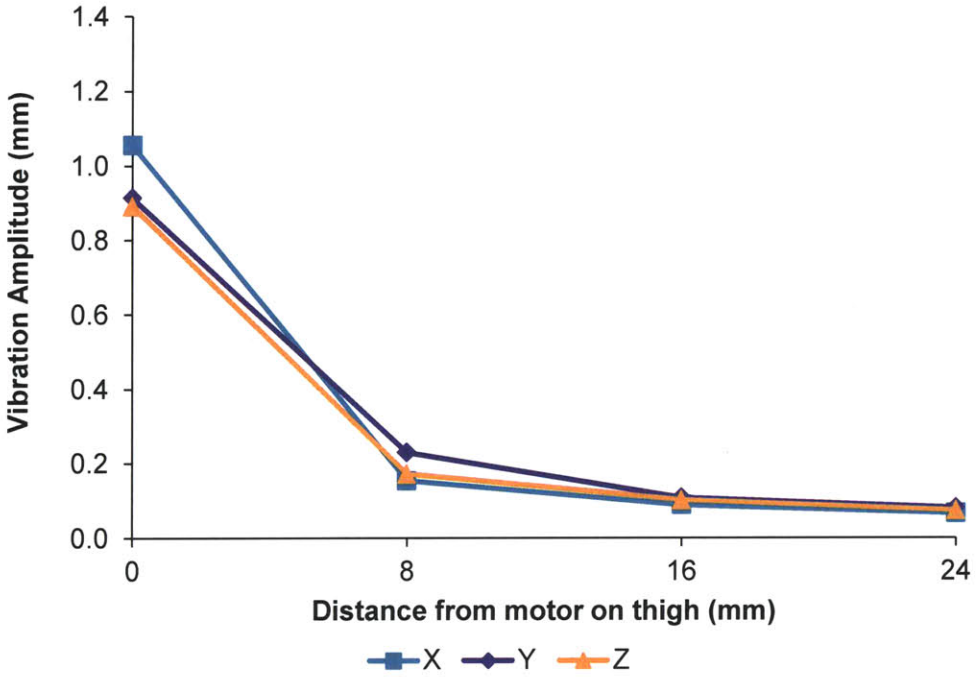

Figure 17. Surface wave amplitude as a function of distance from the motor along the thigh in each axis of acceleration.

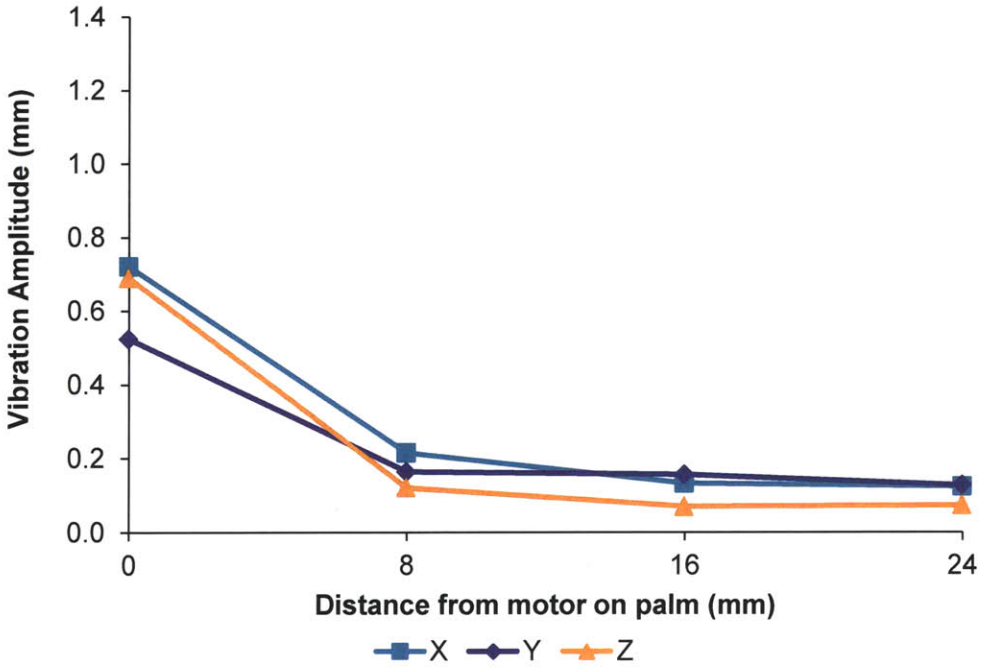

Figure 18. Surface wave amplitude as a function of distance from the motor along the palm in each axis of acceleration.

Figures 16-18 clearly illustrate that although the wave did propagate along the skin for up to 24 mm, it was markedly attenuated within the first 8 mm from the motor. The decrease in amplitude as a percentage of the initial amplitude on the motor is shown for each distance and each body site in Figure 19. The figure shows the percent damping that occurs at each distance and body site, with greater percentages indicating greater attenuation (reduction). From Figure 19 as well as from Figures 16-18 it is evident see that the average attenuation was greater for more compliant body sites such as the thigh (85%) and forearm (78%), and least on the palm (71%). From these results it appears that the surface wave amplitude is closest to being fully damped on the thigh, but is still detectable on all three body sites at 24 mm.

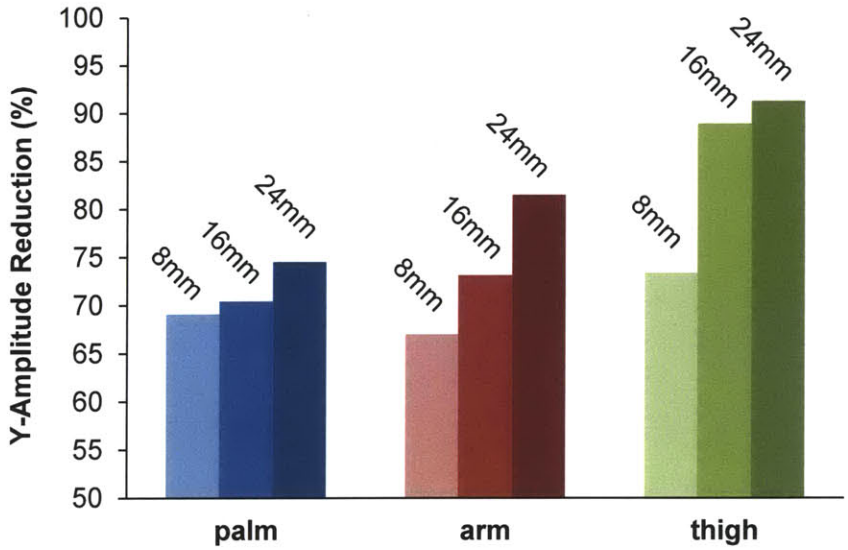

Figure 19. Decrease in amplitude with distance as a percentage of the initial amplitude measured at each site. Values based on 3 V data.

4.3 Bi-directional Experiments

The results of the uni-directional experiment indicated that a further study was required to measure wave amplitudes along the skin in two directions, proximal-distal (longitudinal) and medial-lateral (transverse), to see if any anisotropies in the skin could account for the variations in X and Y-axis acceleration values.

4.3.1 Experimental Methods

Eight subjects, four males and four females, aged 19 to 31 years old were tested. Measurements were made at three body locations—the palm of the hand, the volar surface of the forearm, and the inner thigh—and at three distances from the motor—8 mm, 16 mm and 24 mm. Measurements were taken in two directions along the skin, proximal-distal (longitudinal) and medial-lateral (transverse), at all three body sites. The pancake motor was activated at 3 V during data collection, and each measurement lasted 10 sec with five repetitions. The procedure for data collection was the same as previously described in Section 4.2.1, except that all measurements for the bi-directional tests were collected at a 180 Hz sample rate per axis. The data were analyzed using SPSS to determine if there were any statistically significant effects of direction on the skin, body site, and distance, on the amplitude of vibration measured.

4.3.2 Results

Surface waves produced by activating the motor at 3 V were measured along the skin in two directions on the palm, forearm, and thigh. The measurements were analyzed using the same procedure as that described in Section 4.2.1. Statistical analyses of the surface wave amplitudes using a 3-way repeated measures ANOVA showed there to be a significant effect of distance (X-axis: $F(3,21)=63.51$, $p<0.001$; Y-axis: $F(3,21)=215.12$, $p<0.001$; Z-axis: $F(3,21)=149.97$, $p<0.001$), a significant effect of body site (X-axis: $F(2,14)=31.96$, $p<0.001$; Y-axis: $F(2,14)=18.73$, $p<0.005$; Z-axis: $F(2,14)=19.70$, $p<0.005$), and a significant interaction between distance and body site (X-axis: $F(6,42)=21.99$, $p<0.001$; Y-axis: $F(6,42)=13.92$, $p<0.005$; Z-axis: $F(6,42)=21.51$, $p<0.001$). This interaction of distance and body site is probably due to the notable difference in amplitude attenuation on the palm as opposed to the arm and thigh, as well as the difference in motor amplitudes on the palm versus the arm and thigh in the X and Z axes and the distinguishable amplitudes for all body sites and distances in the Y axis. There was no significant effect of direction (longitudinal vs. transverse) on the amplitudes measured, and no significant interaction between direction and body site or direction and distance. Figure 20 shows the graphs of the bi-directional data plotted for each axis of acceleration at the three body sites in the transverse and longitudinal test directions.

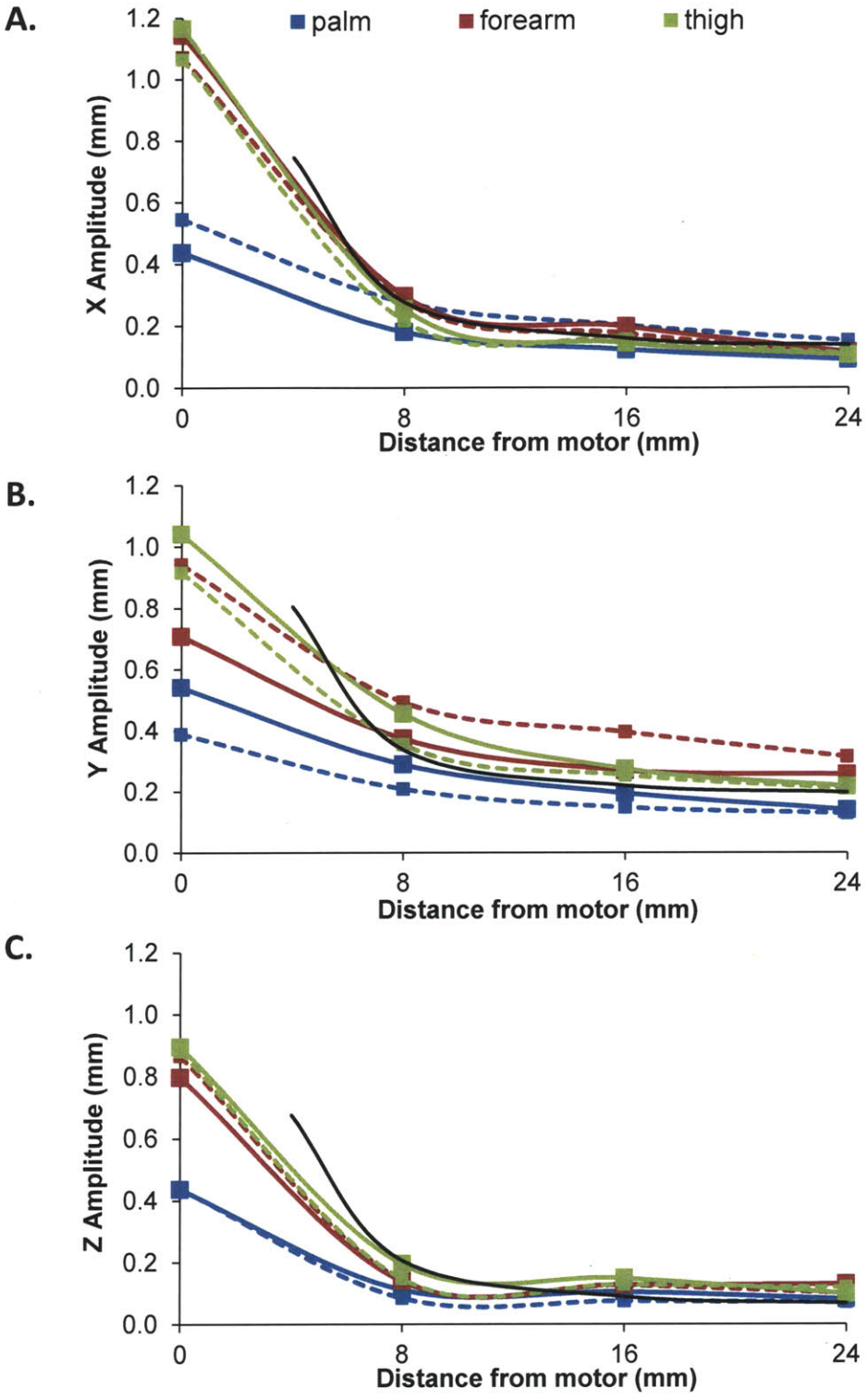

Figure 20 a-c. Surface waves in the X, Y, Z-axis (Figures A, B, and C respectively) as a function of distance traveled at the three body sites in the longitudinal (solid lines) and transverse (dashed lines) directions. The black line indicates a $10/d^2$ fit where d is the distance from the motor.

From Figure 20a-c, it can be seen that the surface wave is propagated mainly in the Y-axis of acceleration, as demonstrated by the higher displacement amplitudes measured in the Y-axis at varying distances from the motor. In both the X and Z axes there is marked attenuation with distance, which would be expected given the configuration of the accelerometer array with respect to the motor. Overall, the results of the bi-directional tests agree with the results found during uni-directional testing. Vibrotactile stimulation of the palm produces the smallest amplitudes and the thigh had the largest. Average wave amplitude attenuation values again showed that the thigh had the highest overall rate of attenuation (80%) in both directions along the skin followed by the arm (75%) and then the palm (71%).

4.4 Discussion

The general trends in the data are consistent in the uni-directional and bi-directional experiments. Both sets of data show that at 24 mm away from the motor there is still a measureable surface wave whose amplitude is greater than the threshold for detecting vibration. This suggests that if a tactile display is used for precise spatial localization then the motors should be spaced at more than 24 mm apart in order to ensure accurate localization. Both experiments also show that body site and distance are significant factors that affect the amplitude of the surface wave, indicating that the surface waves attenuate in a different manner depending on body site. Therefore the optimum motor spacing may also vary as a function of body site. The similar amplitude values on the forearm and thigh, as compared to the palm, probably reflects the difference between hairy and glabrous skin. It is known that hairy skin is less stiff than glabrous skin (Sandford et al., 2012) which can cause lower damping parameters.

The results of the bi-directional tests did not show any significant anisotropies on the skin, as indicated by the absence of any effect of direction (longitudinal versus transverse), in the statistical analyses. Although the skin is known to be anisotropic, these results are consistent with previous findings by Liang and Boppart (2010), who found that there were no measureable anisotropies in skin stiffness when measured parallel and orthogonal to the Langer lines at low frequencies of around 50 Hz. Anisotropies in skin stiffeness did not appear until the skin was tested at much higher frequencies of around 600 Hz. The simple function ($10/d^2$) fitted to the data in Figure 20a-c illustrates that the decrease in vibrational amplitude occurs at a rate roughly proportional to the inverse square of distance traveled, as has been previously found (Franke et al., 1951) illustrating that the rate of amplitude decrease is roughly proportional to the inverse square of distance traveled.

5. Psychophysical experiments

The final experiment was a psychophysical experiment aimed at testing subjects' ability to localize the site of vibrotactile stimulation in a tactile display. The objective was to see how well subjects could identify the location of the source of vibration in an array of nine motors, and to determine whether localization accuracy varied as a function of the site on the body where the array was mounted. At each location two spacing configurations were tested. The results of this psychophysical experiment could then be interpreted with respect to the surface wave measurements made in the earlier experiments.

5.1 Methods

This experiment tested eight subjects, four males and four females, ages 19 to 31. A three-by-three array of pancake motors was taped to the skin in the same three body locations as used in the previous experiments: the palm, the volar forearm, and the thigh. At each location the motors were placed in two spacing configurations, 8 mm and 16 mm apart edge-to-edge within the three-by-three array configuration. All subjects were tested at all skin sites and spacings with the order of presentation randomized across subjects. The test setup is shown for the palm in Figure 21.

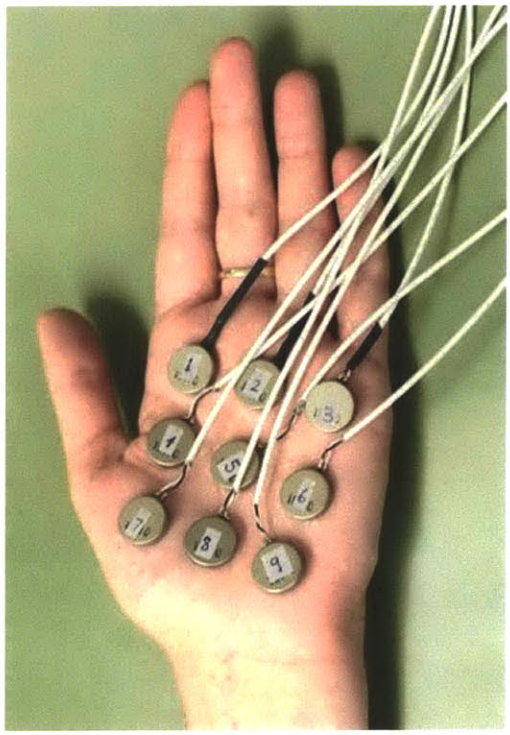

Figure 21. 3x3 motor array setup on the palm for psychophysical testing with an inter-motor spacing of 8 mm.

During testing, one motor was activated with a 500 msec pulse at 3.3 V. Every motor was activated on average three times for a total of 27 trials at each site and distance. After each motor was activated subjects had to identify which motor they thought was activated by entering the motor number, one though nine, on a keyboard. Subjects were not allowed to see the motor array during testing and were given an answer selection sheet, which showed the location of each motor, to use as a reference (see Figure 22). In all tests the top row containing motors 1-3 was in the most distal position, and the columns of the array (motors 1-4-7, 2-5-8, and 3-6-9) were along the longitudinal (proximal-distal) axis of the limbs. After testing was completed, each subject's answers were scored and entered into a response matrix so that errors could be analyzed in addition to correct responses.

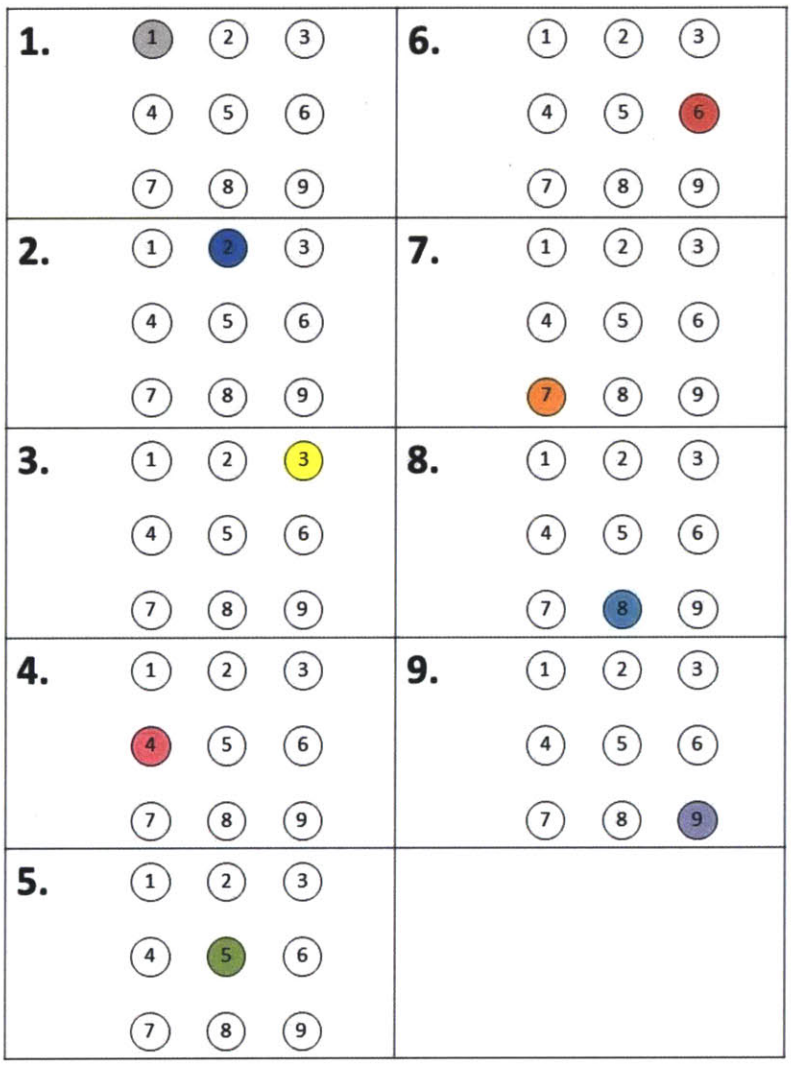

Figure 22. Answer selection sheet shown to subjects during psychophysical testing showing the location of each possible motor vibration.

5.2 Results

The mean percent correct values were calculated for each experimental condition and are shown graphically in Figure 23. The accuracy on the palm increased from 79% (SD: 17%) correct to 83% (SD: 21%) correct when the spacing between the motors increased from 8 mm to 16 mm. For the forearm, the improvement was similar (45% (SD: 18%) to 53% (SD: 18%) correct), although overall performance was much poorer. For the thigh, localization accuracy deteriorated as the spacing between the motors increased (from 48% (SD: 10%) to 43% (SD: 11%) correct).

A two-way repeated measures ANOVA with body site and inter-motor spacing as factors revealed that body site had a significant effect on percent correct scores ($F(2,14)=25.21$, $p<0.001$) but that the spacing of the motors was not significant. There was no significant interaction between body site and spacing. Half of the subjects were presented with the 8 mm spacing first and half with the 16 mm spacing first, statistical analysis confirmed that the order of presentation did not have a significant effect on performance ($F(1,7)=2.07$, $p>0.15$).

Table 2. Percent correct scores from the localization experiment for each subject and test configuration.

Subject	Palm 8	Palm 16	Arm 8	Arm 16	Thigh 8	Thigh 16
A	93%	100%	70%	78%	59%	52%
B	85%	96%	44%	78%	59%	48%
C	96%	100%	70%	56%	37%	37%
D	81%	74%	33%	42%	33%	25%
E	45%	44%	30%	40%	52%	52%
F	88%	100%	41%	56%	56%	52%
G	78%	89%	52%	44%	41%	48%
H	67%	63%	22%	30%	44%	30%
Mean	**79%**	**83%**	**45%**	**53%**	**48%**	**43%**
Std. Dev.	17%	21%	18%	18%	10%	11%

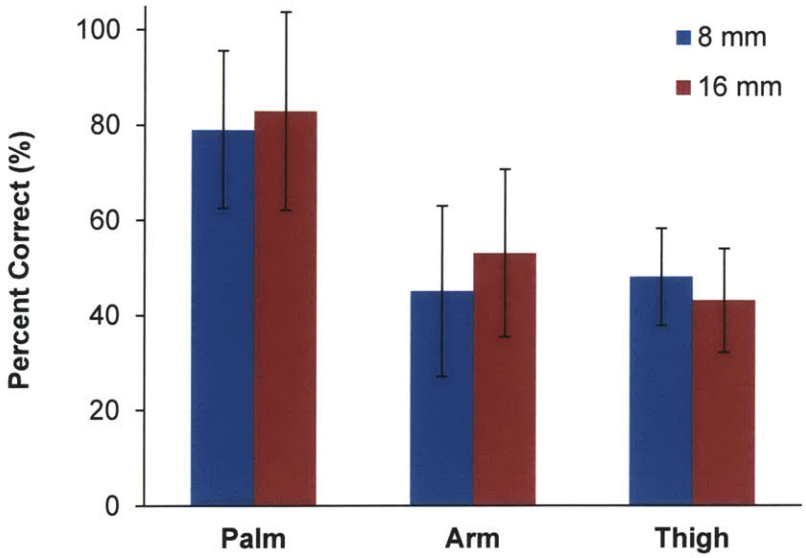

Figure 23. Mean percent correct scores when identifying the location of a motor on the palm, forearm, and thigh with motor array spacing of 8 mm and 16 mm. Standard deviations are shown.

From the results displayed in Table 2 it can be seen that although the mean percent correct for the palm at 16 mm spacing was only 83%, three subjects achieved a perfect score (100%), with a fourth subject scoring 96% correct with only one incorrect response. Further review of Table 2 shows that only about half of the subjects scored above 50% correct on the arm (3 subjects at 8 mm, and 4 subjects at 16 mm) and on the thigh (4 subjects at 8 mm, and 3 subjects at 16 mm). At all sites, there is considerable variability among subjects, with some subjects performing better when the motors were spaced at 8 mm, and others better with 16 mm spacing. For some subjects the spacing between motors had little effect on performance.

The confusion matrix of the subjects' responses can provide insight into the factors that may have influenced localization accuracy. An initial analysis of the errors revealed that subjects were able to identify the correct column of activation nearly twice as often as the correct row, averaging 59% correct column identification as compared to 26% correct row identification. Figure 24 shows the average percent of correct row and column identification for each body site and spacing. When looking at how often an adjacent motor was chosen, an adjacent motor in the same column was still chosen twice as frequently (55%) as an adjacent motor in the same row (25%). Of the remaining 20%, an average of 13% of incorrect responses selected a diagonally adjacent motor, leaving only about 3% of all incorrect responses as not being in the correct column, row, or diagonally adjacent.

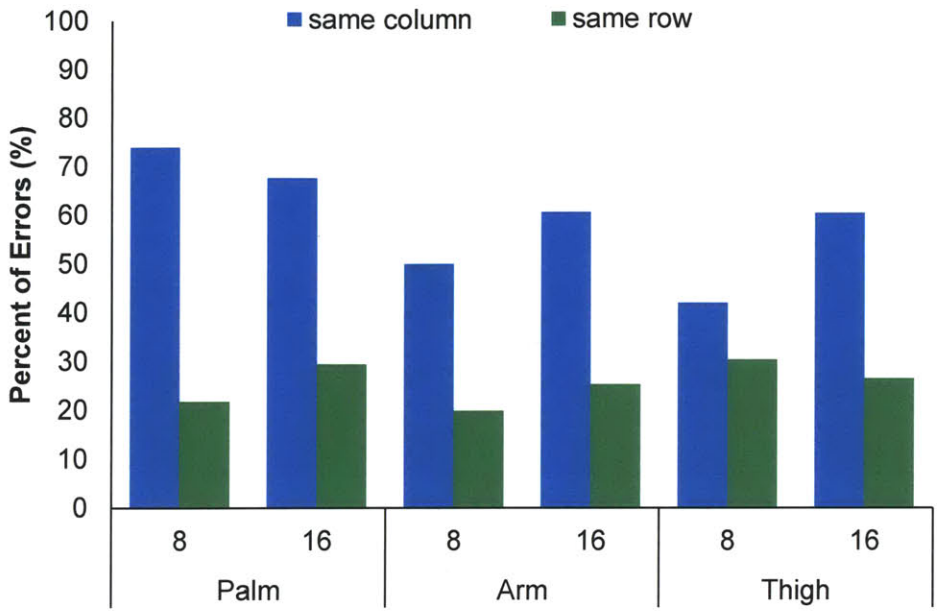

Figure 24. Mean percent of errors in which the correct row or column of the activated motor was identified.

From the confusion matrix the information transfer associated with the various skin sites was calculated. Information Transfer (IT) values determine how many "bits" of information subjects can distinguish from the set of stimuli presented. "The quantity IT measures the increase in information about the signal transmitted resulting from knowledge of the received signal" (Tan et al., 2010, p. 99). For each stimulus-response pair (S_i, R_j) the IT was calculated by:

$$IT(S_i, R_j) = \log_2\left(\frac{P(S_i/R_j)}{P(S_i)}\right),$$

where $P(S_i/R_j)$ is the proportion of correct responses R_j for S_i, and $P(S_i)$ is the probability of stimulus S_i. The average IT value for each skin site and spacing was calculated using the equation:

$$IT = \sum_{j=1}^{K}\sum_{i=1}^{K} P(S_i, R_j)\log_2\left(\frac{P(S_i/R_j)}{P(S_i)}\right) = \sum_{j=1}^{K}\sum_{i=1}^{K} P(S_i, R_j)\log_2\left(\frac{P(S_i,R_j)}{P(S_i)P(R_j)}\right),$$

where $P(S_i, R_j)$ is the probability of response R_j given S_i, and $P(R_j)$ is the probability of R_j. The maximum IT is called the Information in Stimulus (IS) which is the total number of bits contained in the stimuli or the IT value for 100% accuracy, and can be calculated more simply using the equation:

$$IS = -\sum_{i=1}^{K} P(S_i)\log_2 P(S_i)$$

The IS, or maximum IT, for this set of stimuli assuming 27 trials for each of the eight subjects, in which each motor is stimulated exactly three times, is 3.17 bits, meaning that there are 3.17 total possible bits of information to be transferred from the stimuli with nine locations to be identified. The calculation 2^{IT} gives the maximum number of locations that can be correctly identified (Chen et al., 2008). Given this, the IT values for the palm at 8 and 16 mm were 2.34 bits (5 locations) and 2.46 bits (5.5 locations). On the forearm the IT was 1.02 bit (2 locations) and 1.42 bits (2.7 locations) for 8 and 16 mm, and on the thigh the IT was 1.17 bits (2.2 locations) and 1.32 bits (2.5 locations) respectively. This shows that the poorest performance was actually on the forearm with an inter-motor spacing of 8 mm, contrary to percent correct scores which show the thigh at 16 mm as having the lowest accuracy. The IT values also show that there is improvement with increased spacing on all three body parts. Figure 25 shows a plot of these IT values as compared to the maximum IT value shown by the dashed line.

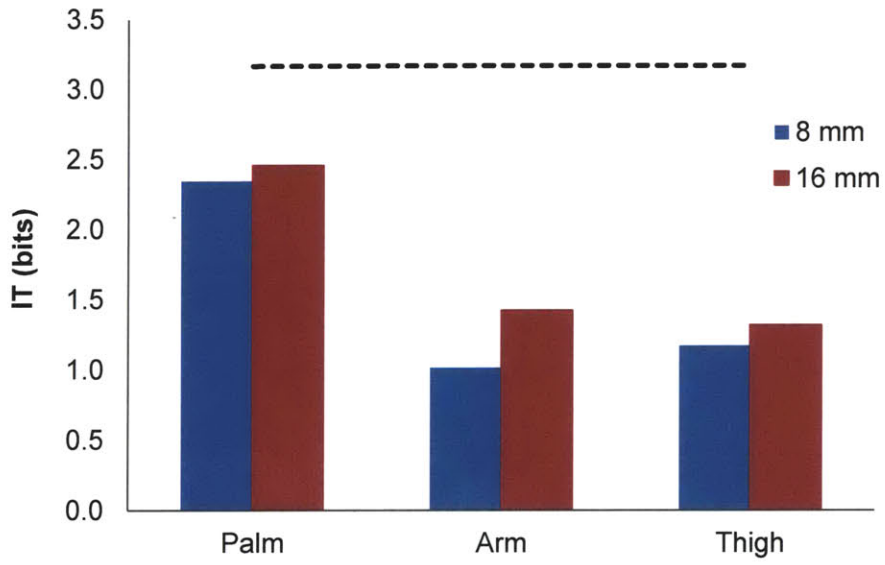

Figure 25. Information Transfer (IT) values for each body site and spacing compared to the maximum possible IT value for these stimuli.

It was of interest to determine whether there were any differences due to gender in the ability to localize a point of stimulation on the skin. When performance was analyzed over all three body sites, it was found that the female subjects consistently scored higher than the males by an average of about 25% on both the palm and forearm and 10% on the thigh. The mean percent correct scores of males and females at each body site and spacing are shown in Figure 26. Average IT for males and females, as

shown in Figure 27, illustrates the same trend of better female performance. Since only eight subjects participated in these experiments, there are not enough subjects to analyze these data statistically. Additional subjects would be needed in order to determine if the effects are robust.

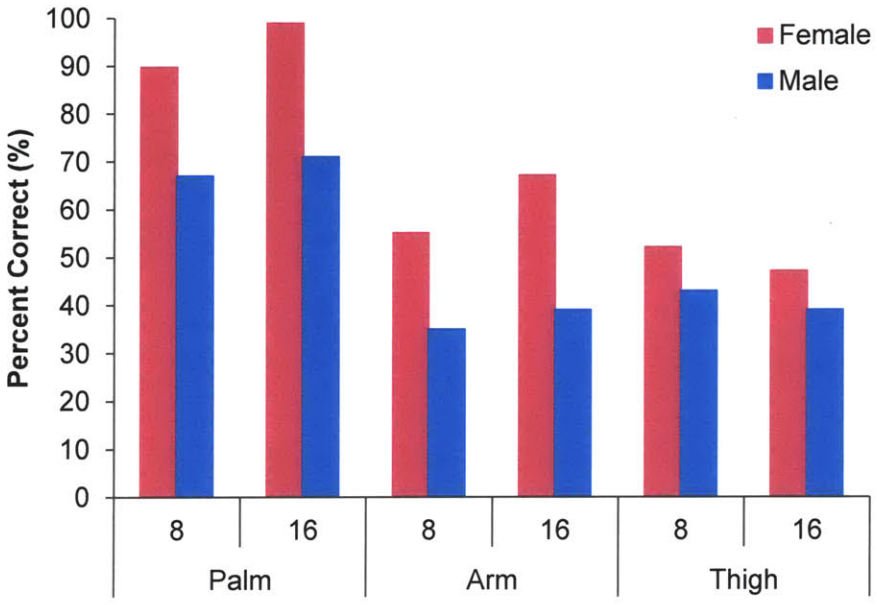

Figure 26. Percent correct scores for males and females as a function of body site and motor spacing.

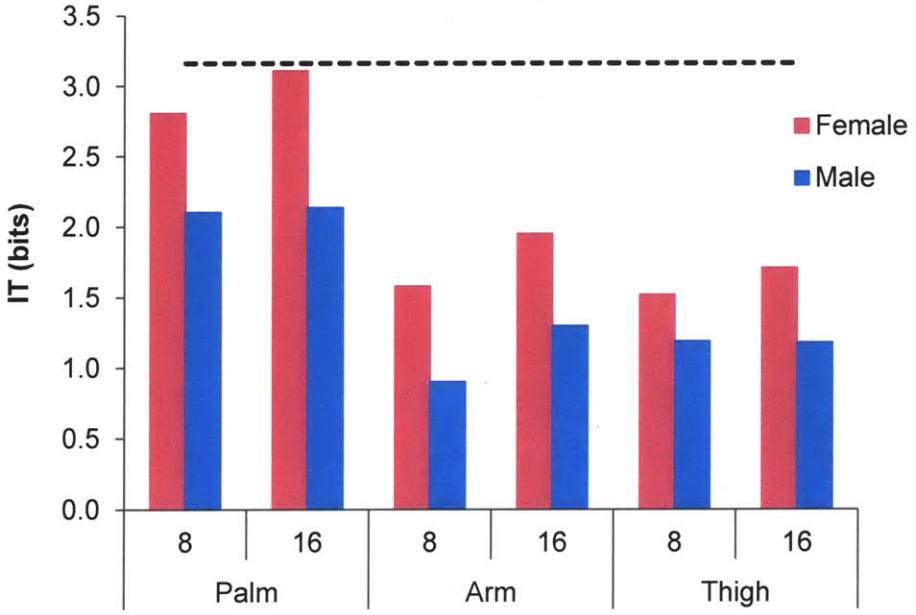

Figure 27. Average Information Transfer (IT) values for males and females for each body site and spacing density compared to the maximum possible IT value for these stimuli.

To determine subjects' ability to identify specific motor locations, the percentage of correct responses were averaged across all six combinations of body parts and spacing. The results are displayed in Figure 28. From these compiled results it can be seen that the four corner motors (motor 1, 3, 7, and 9) were most often correctly identified with a mean identification rate of 66% (SD: 5%) as compared to 52% (SD: 4%) for the remaining five motors. Motor 1 and 7 had the highest overall identification (70%) across all responses, followed by motor 9 (64%) and motor 3 (61%).

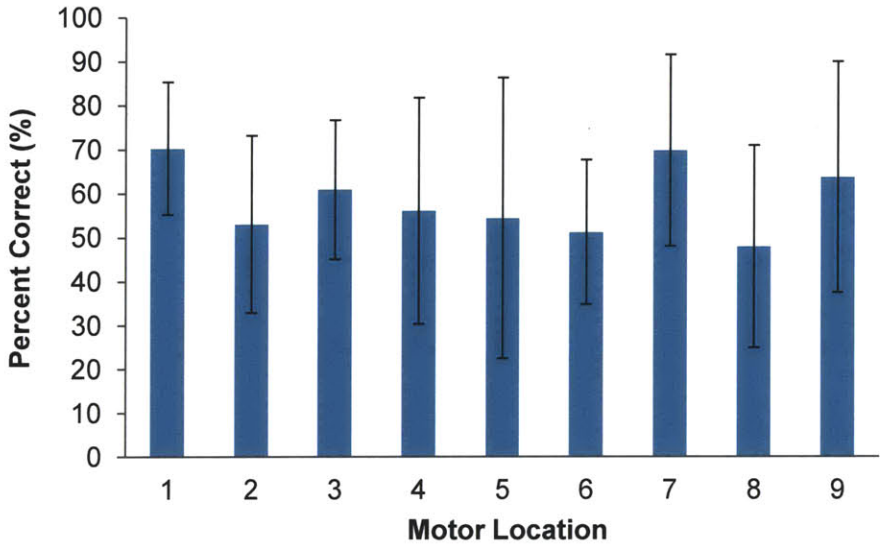

Figure 28. Percent correct scores for each motor location averaged across all body sites and spacing densities. Standard deviations are shown.

5.3 Discussion

The results of the psychophysical experiments indicate that a vibrotactile display mounted in the forearm or thigh requires an inter-motor separation distance of at least 16 mm if it is to be used effectively for spatial cuing. However, on the palm, a 16 mm inter-motor spacing seems to be sufficient to achieve high localization accuracy, although accuracy would surely increase with greater separation. The key limitation on the palm is the small surface area available to mount a display. In order to increase the inter-motor pacing on the palm the number of motors must be reduced. Using fewer motors may be beneficial in general since the IT results indicate that only two locations could be accurately identified on the forearm and thigh, and that only five out of nine locations could be identified on the palm. This is consistent with previous research performed on the wrist by Chen et al. (2008) in which IT analyses revealed that in a three-by-three array with 25 mm inter-motor spacing only

two locations could be accurately identified by two out of three subjects, whereas the third subject could locate four motors. Our finding that the column of activation was more often identified than the row, is also consistent with previous studies which have found the tactile localization is best across the medial-lateral axis as opposed to the proximal-distal axis (Chen et al., 2008; Gibson & Craig, 2005; Jones et al., 2009).

As in Cholewiak and Collins' (2003) research we would expect to see an improvement in localization accuracy as the spacing of the motors increased. However, we only observed this positive correlation of localization accuracy and increased spacing on the palm and forearm, and not on the thigh. When comparing IT we see that Cholewiak and Collins' values of 1.28 bits to 1.67 bits (out of a total possible 2.81 bits) at 25 and 50 mm inter-motor spacing, are consistent with our results of 1.02 bits and 1.42 bits for 8 and 16 mm motor spacing on the forearm, and 1.17 bits and 1.32 bits on the thigh (out of a possible 3.17 bits). Comparison of information transfer values shows that there is not much improvement in localization accuracy as the inter-motor spacing increases from 16 to 25 mm. The IT values at 16 mm in the present experiment were even slightly greater than those of Cholewiak and Collins, which might be attributed to the higher frequency of activation of their motors which may cause surface waves to propagate further along the skin.

6. Conclusions and Future Work

The results from this research showed that surface waves induced by motor vibration on the skin could be detected 24 mm away from the motor with amplitudes that are higher than the threshold for vibrotactile detection. This indicates that tactors should be spaced more than 24 mm apart in order to ensure accurate vibrotactile localization. Previous research by Jones and Held (2008) found that surface waves were detectable up to distances of 60 mm on a skin-like substrate, suggesting that motors should be spaced at least 60-80 mm apart to for accurate tactile localization. However, the results of the present psychophysical experiments indicate that the spacing between motors can be much less than this on the palm of the hand, given that subjects achieved accuracy rates of 79% to 83% at distances as small as 8 and 16 mm. On the forearm and thigh the psychophysical results showed that the spacing between motors should be greater than 16 mm for accurate localization and most likely greater than 24 mm as indicated by the accelerometer measurements. The small receptive fields in the glabrous skin of the palm presumably allows the origin of traveling surface waves to be well localized, despite perceivable amplitudes traveling up to 24 mm away from the source. Conversely, the broader receptive fields on the forearm and thigh are associated with poorer spatial acuity, and therefore less accurate localization. From these results we can conclude that the best location for communicating high accuracy spatial localization cues is on the palm of the hand, especially when trying to minimize the overall size of a tactile display.

From the present research and previous results it appears that several factors may improve the localization accuracy of a vibrotactile display. Rather than merely increasing the overall spacing between motors, a more effective strategy would be to space motors with respect to the anatomical axes. Tactor spacing along the medial-lateral axis in an orientation that straddles the center proximal-distal axis is more effective than equal spacing oriented along longitudinal axis. For example, patterns that move across the forearm are more easily identified than ones that vary along the longitudinal (proximal-distal) axis of the arm (Jones et al., 2009). In addition, motors are more easily identified by their medial-lateral placement (column of activation) than their proximal-distal location (row of activation) (Chen et al., 2008). Another important design consideration that may lead to improved localization accuracy is placement of the motors on or around anatomical "landmarks." Localization accuracy may also be improved by changing the input signal, either by using a more isolated one-dimensional stimulus or by reducing the stimulus frequency and amplitude, given that smaller initial amplitudes will be damped out over a shorter distance.

Further investigation using the current motors should replicate the bi-directional accelerometer experiments, collecting measurements over a greater distance along the skin to see how long it takes for the surface wave to attenuate to imperceptible amplitudes. Bi-directional experiments should also be performed using motors that can be activated at much higher frequencies and with a greater number of subjects to see if there are any anisotropies in the transmission of surface waves on the skin. For all accelerometer measurements, a newly configured more adaptable accelerometer array may also be desirable so that the size of the array is limited to the number of accelerometers needed for taking measurements. Future research should also try to increase sampling rates to allow for simultaneous sampling of more accelerometers and at higher frequencies. Future work should also explore different tactor types, to see how the mechanical stimuli produced by these tactors travel along the skin.

Further psychophysical experiments using the same motors should be performed with greater inter-motor spacing, such as 24 mm and more. These experiments could also look into the effect of reducing the total number of motors in an array, such as using a two by two array with the same overall dimensions as previously tested. Psychophysical experiments should also test arrays with different inter-motor spacing along the two anatomical axes (medial-lateral and proximal-distal) in order to find the distance ratio required for equal vibrotactile localization accuracy along each axis.

In summary, measurements of the properties of surface waves induced by vibrotactile stimulation and the accuracy of locating a point of stimulation at three locations on the body (the palm, forearm, and thigh) were made and analyzed to determine the optimal configuration of vibrotactile displays on different parts of the body. For the same motor output, the measured frequency and amplitude of vibration varied as a function of skin site. The frequency was higher and the amplitude was lower on the palm as compared to the volar forearm and thigh. Although surface waves attenuated more rapidly on the thigh than the forearm the ability to localize stimulation on was slightly greater on the forearm then thigh. The most accurate localization was found on the palm, consistent with its high spatial acuity. Overall, both the mechanical and psychophysical experiments showed a significant difference in the behavior of glabrous and hairy skin, showing that glabrous skin is better-suited for tactile localization cues.

References

Bolanowski, S. J., Gescheider, G. A., & Verrillo, R. T. (1994). Hairy skin: Psychophysical channels and their physiological substrates. *Somatosensory and Motor Research, 11*(3), 279-290.

Bolanowski, S. J., Gescheider, G. A., Verillo, R. T., & Checkosky, C. M. (1988). Four channels mediate the mechanical aspects of touch. *Journal of the Acoustical Society of America, 84*(5), 1680-1694.

Boyer, G., Zahouani, H., Le Bot, A., & Laquieze, L. (2007). In vivo characterization of viscoelastic properties of human skin using dynamic micro-indentation. *29th Annual International Conference of the IEEE EMBS*, (pp. 4584-4587). Lyon, France.

Chen, H.-Y., Santos, J., Graves, M., Kim, K., & Tan, H. Z. (2008). Tactor localization at the wrist. In M. Ferre (Ed.), *EuroHaptics, LNCS. 5024*, pp. 209-218. Madrid, Spain: Springer Berlin / Heidelberg.

Cholewiak, R. W., & Collins, A. A. (2003). Vibrotactile localization on the arm: Effects of place, space and age. *Perception & Psychophysics, 65* (7), 1058-1077.

Cholewiak, R. W., Collins, A. A., & Brill, C. (2001). Spatial factors in vibrotactile pattern perception. *EuroHaptics*, (pp. 41-48). Birmingham.

Franke, E. K., von Gierke, H. E., Oestreicher, H. L., & von Wittern, W. W. (1951). *The Propagation of Surface Waves Over the Human Body.* Dayton, Ohio: United States Air Force.

Gardner, E. P., & Martin, J. H. (2000). Coding of sensory information. In E. R. Kandel, J. H. Schwartz, & T. M. Jessell (Eds.), *Principles of Neural Science* (4th ed.). New York: McGraw-Hill.

Gardner, E. P., Martin, J. H., & Jessell, T. M. (2000). The Bodily Senses. In E. R. Kandel, J. H. Schwartz, & T. M. Jessell (Eds.), *Principles of Neural Science* (4th ed.). New York: McGraw-Hill.

Gescheider, G. A., Bolanowski, S. J., Hall, K. L., Hoffman, K. E., & Verrillo, R. T. (1994). The effects of aging on information-processing channels in the sense of touch: I. Absolute sensitivity. *Somatosensory and Motor Research, 11*(4), 345-357.

Gibson, G. O., & Craig, J. C. (2005). Tactile spatial sensitivity and anisotropy. *Perception & Psychophysics, 67*(6), 1061-1079.

Guinan, A. L., Koslover, R. L., Caswell, N. A., & Provancher, W. R. (2012). Bi-manual skin stretch feedback embedded within a game controller. *IEEE Haptics Symposium*, (pp. 255-260). Vancouver, BC.

Johansson, R. S., & Vallbo, A. B. (1979). Tactile sensibility in the human hand: Relative and absolute densities of four types of mechanoreceptive units in glabrous skin. *Journal of Physiology, 286*, 283-300.

Jones, L. A., & Held, D. A. (2008). Characterization of tactors used in vibrotactile displays. *Journal of Computing and Information Science in Engineering, 8*, 044501-1 - 044501-5.

Jones, L. A., & Sofia, K. O. (2012). Measuring surface wave propagation during vibrotactile stimulation. *IEEE Haptics Symposium* , (pp. 457-461). Vancouver, BC.

Jones, L. A., Held, D., & Hunter, I. (2010). Surface waves and spatial localization in vibrotactile displays. *IEEE Haptics Symposium*, (pp. 91-94). Waltham, MA.

Jones, L. A., Kunkel, J., & Piateski, E. (2009). Vibrotactile pattern recognition on the arm and back. *Perception, 38*, 52-68.

Konietzny, F., & Hensel, H. (1977). Response of rapidly and slowly adapting mechanoreceptors and vibratory sensitivity in human hairy skin. *Pflügers Archiv European Journal of Physiology, 368*, 39-44.

Li, C., Guan, G., Reif, R., Huang, Z., & Wang, R. K. (2012). Determining elastic properties of skin by measuring surface waves from an impulse mechanical stimulus using phase-sensitive optical coherence tomography. *Journal of the Royal Society Interface, 9*(70), 831-841.

Liang, X., & Boppart, S. A. (2010). Biomechanical properties of in vivo human skin from dynamic optical coherence elastography. *IEEE Transactions on Biomedical Engineering, 57*(4), 953-959.

Morioka, M., Whitehouse, D. J., & Griffin, M. J. (2008). Vibrotactile thresholds at the fingertip, volar forearm, large toe, and heel. *Somatosensory and Motor Research, 25*(2), 101-112.

Salzer, Y., Oron-Gilad, T., & Ronen, A. (2010). Vibrotactor-Belt on the Thigh – Directions in the Vertical Plane. *EuroHaptics, LNCS* (pp. 359-364). Springer-Verlag Berlin Heidelberg.

Sandford, E., Chen, Y., Hunter, I., Hillebrand, G., & Jones, L. (In press 2012). Capturing skin properties from dynamic mechanical analyses. *Skin Research and Technology*.

Saunders, F. A. (1973). An electrotactile sound detector for the deaf. *IEEE Transactions on Audio and Electroacoustics, AU-21*(3), 285-287.

Stevens, J., & Choo, K. (1996). Spatial acuity of the body surface over the life span. *Somatosensory and Motor Research, 13*(2), 153- 166.

Tan, H. Z., Reed, C. M., & Durlach, N. I. (2010). Optimum information transfer rates for communication through haptic and other sensory modalities. *IEEE Transactions on Haptics, 3*(2), 98-108.

van Erp, J. B. (2007). *Tactile Displays for Navigation and Orientation: Perception and Behavior.* Ph.D., Utrecht University, The Netherlands.

Wall, C., & Weinberg, M. S. (2003). Balance prostheses for postural control: Preventing falls in the balance impaired by displaying body-tilt information to the subject via an array of tactile vibrators. *IEEE Engineering in Medicine and Biology Magazine*, 84-90.

Appendix 1. PCB Components and Construction Specs

Circuit construction by Flex Interconnect Technologies:

>1 mil kapton

>1 mil adhesive

>1 oz copper

>1 mil adhesive

>1 mil kapton

>1 mil adhesive

>1 oz copper

>1 mil adhesive

>1 mil kapton

Surface finish for exposed copper: Tin Lead HASL

Qty. per PCB	Reference Destination	Manufacturer Part #	Manufacturer	Description	Package	Type
8	A0,A1,A2,A3, A4,A5,A6,A7	LIS331DLH	STMicroelectronics	STMicro. 3-axis Accelerometer ±2g/±4g/±8g, 2.5V	LGA16	fine pitch
8	T0,T1,T2,T3,T 4,T5,T6,T7	TLCK106M006QTA	AVX Corporation	CAP TANT 10UF 6.3V 20% 0402 SMD, POLARIZED	0402 (1005 Metric)	surface mount
8	C0,C1,C2,C3, C4,C5,C6,C7	CC0603ZRY5V7BB1 04	Yageo (VA)	CAP CERAMIC .1UF 16V Y5V 0603	0603 (1608 Metric)	surface mount
1	U1	LP2985AIM5-3.3/NOPB	National Semiconductor	IC REG LDO MICROPOWER SOT23-5	SOT-23 5-Lead	surface mount

Appendix 2. Mean Responses from Psychophysical Experiments

Confusion matrices showing results of psychophysical test responses, showing how often each motor was correctly identified and how often different motors were chosen. The rows indicate which motor was stimulated and the columns indicate the response entered by subjects. The diagonal from upper left to lower right shows the percentage that each motor was correctly identified. Next to the title of each matrix indicating the body site and spacing, is the percentage of average correct responses.

Palm 8 (Avg. correct 78%)

stimuli \ responses	1	2	3	4	5	6	7	8	9
1	72%	12%	0%	16%	0%	0%	0%	0%	0%
2	0%	58%	0%	0%	38%	4%	0%	0%	0%
3	0%	0%	69%	0%	0%	27%	0%	0%	4%
4	8%	0%	0%	84%	0%	0%	8%	0%	0%
5	0%	0%	0%	0%	100%	0%	0%	0%	0%
6	0%	0%	6%	0%	0%	67%	0%	0%	28%
7	0%	0%	0%	8%	0%	0%	92%	0%	0%
8	0%	0%	0%	4%	0%	0%	29%	67%	0%
9	0%	0%	0%	0%	0%	4%	0%	0%	96%

Palm 16 (Avg. correct 84%)

stimuli \ responses	1	2	3	4	5	6	7	8	9
1	100%	0%	0%	0%	0%	0%	0%	0%	0%
2	0%	83%	4%	0%	13%	0%	0%	0%	0%
3	0%	0%	71%	0%	0%	19%	0%	0%	10%
4	4%	0%	0%	92%	4%	0%	0%	0%	0%
5	0%	0%	0%	4%	92%	0%	0%	4%	0%
6	0%	0%	4%	0%	0%	72%	0%	0%	24%
7	0%	0%	0%	13%	0%	4%	83%	0%	0%
8	0%	0%	0%	0%	0%	0%	20%	76%	4%
9	0%	0%	0%	0%	0%	8%	0%	4%	88%

Arm 8 (Avg. correct 45%)

stimuli \ responses	1	2	3	4	5	6	7	8	9
1	64%	4%	0%	16%	8%	0%	8%	0%	0%
2	8%	25%	4%	8%	33%	0%	8%	8%	4%
3	0%	0%	36%	5%	14%	27%	0%	5%	14%
4	21%	8%	0%	42%	8%	0%	17%	4%	0%
5	8%	13%	4%	8%	33%	4%	8%	17%	4%
6	0%	0%	5%	0%	14%	33%	0%	19%	29%
7	0%	0%	0%	12%	4%	0%	84%	0%	0%
8	0%	0%	0%	13%	17%	8%	13%	42%	8%
9	0%	8%	0%	0%	8%	13%	4%	21%	46%

Arm 16 (Avg. correct 53%)

stimuli \ responses	1	2	3	4	5	6	7	8	9
1	60%	8%	0%	24%	4%	4%	0%	0%	0%
2	13%	38%	4%	4%	33%	4%	0%	4%	0%
3	0%	0%	45%	0%	5%	32%	0%	0%	18%
4	25%	13%	0%	50%	0%	0%	13%	0%	0%
5	0%	8%	4%	4%	32%	28%	4%	12%	8%
6	0%	0%	16%	0%	0%	53%	0%	0%	32%
7	0%	0%	0%	24%	0%	0%	72%	0%	4%
8	0%	4%	4%	0%	8%	4%	21%	54%	4%
9	0%	0%	0%	0%	0%	9%	0%	17%	74%

Thigh 8 (Avg. correct 48%)

stimuli \ responses	1	2	3	4	5	6	7	8	9
1	64%	12%	0%	24%	0%	0%	0%	0%	0%
2	19%	54%	15%	4%	4%	4%	0%	0%	0%
3	0%	5%	71%	0%	0%	24%	0%	0%	0%
4	28%	12%	4%	36%	4%	0%	8%	8%	0%
5	4%	16%	4%	4%	44%	0%	12%	12%	4%
6	0%	0%	6%	0%	11%	44%	11%	11%	17%
7	8%	0%	0%	25%	4%	0%	54%	4%	4%
8	0%	0%	4%	8%	8%	16%	28%	32%	4%
9	0%	0%	0%	0%	21%	21%	4%	25%	29%

Thigh 16 (Avg. correct 43%)

stimuli \ responses	1	2	3	4	5	6	7	8	9
1	63%	13%	0%	17%	0%	0%	8%	0%	0%
2	4%	60%	28%	0%	4%	0%	4%	0%	0%
3	0%	0%	71%	0%	0%	19%	0%	0%	10%
4	52%	4%	0%	32%	12%	0%	0%	0%	0%
5	0%	31%	15%	15%	31%	4%	0%	0%	4%
6	6%	0%	17%	0%	22%	33%	0%	0%	22%
7	4%	0%	0%	54%	8%	0%	35%	0%	0%
8	0%	5%	0%	9%	45%	5%	14%	14%	9%
9	0%	0%	0%	4%	8%	23%	0%	15%	50%

Individual subject performance

Subject		Palm 8	Palm 16	Arm 8	Arm 16	Leg 8	Leg 16	
7	(M)	45%	44%	30%	40%	52%	52%	44%
4	(M)	81%	74%	33%	42%	33%	25%	48%
2	(F)	85%	96%	44%	78%	59%	48%	68%
9	(F)	88%	100%	41%	56%	56%	52%	65%
10	(M)	78%	89%	52%	44%	41%	48%	59%
1	(F)	93%	100%	70%	78%	59%	52%	75%
3	(F)	96%	100%	70%	56%	37%	37%	66%
11	(M)	67%	63%	22%	30%	44%	30%	43%
AVG		**79%**	**83%**	**45%**	**53%**	**48%**	**43%**	
Std. Dev.		17%	21%	18%	18%	10%	11%	

		Correct column	Correct row
Palm	8	74%	22%
	16	68%	29%
Arm	8	50%	20%
	16	61%	25%
Thigh	8	42%	30%
	16	60%	26%
Average		**59%**	**26%**

Adjacent Motor Selections		Correct column	Correct row
Palm	8	72%	22%
	16	62%	29%
Arm	8	44%	19%
	16	55%	24%
Thigh	8	40%	29%
	16	55%	26%
Average		**55%**	**25%**

TOTAL Overall accuracy per motor (Avg. 59%)

	1	2	3	4	5	6	7	8	9	Total occurrences
1	70%	8%	0%	16%	2%	1%	3%	0%	0%	148
2	7%	53%	10%	3%	20%	2%	2%	2%	1%	147
3	0%	1%	61%	1%	3%	25%	0%	1%	9%	133
4	23%	6%	1%	56%	5%	0%	7%	2%	0%	148
5	2%	12%	5%	6%	54%	6%	4%	7%	3%	147
6	1%	0%	8%	0%	8%	51%	2%	5%	25%	119
7	2%	0%	0%	23%	3%	1%	70%	1%	1%	149
8	0%	1%	1%	6%	13%	6%	21%	48%	5%	144
9	0%	1%	0%	1%	6%	13%	1%	14%	64%	146

Total responses per motor

56% same column
25% same row

51% Adjacent motor in column
25% Adjacent motor in row
16% Adjacent motor diagonal

Appendix 3. Male vs. Female Mean Responses from Psychophysical Experiments

Palm 8 (Avg. 90%)

FEMALE Responses

stimuli	1	2	3	4	5	6	7	8	9
1	83%	8%	0%	8%	0%	0%	0%	0%	0%
2	0%	58%	0%	0%	42%	0%	0%	0%	0%
3	0%	0%	77%	0%	0%	23%	0%	0%	0%
4	0%	0%	0%	100%	0%	0%	0%	0%	0%
5	0%	0%	0%	0%	100%	0%	0%	0%	0%
6	0%	0%	11%	0%	0%	89%	0%	0%	0%
7	0%	0%	0%	0%	0%	0%	100%	0%	0%
8	0%	0%	0%	0%	0%	0%	0%	100%	0%
9	0%	0%	0%	0%	0%	0%	0%	0%	100%

Palm 8 (Avg. 67%)

MALE Responses

stimuli	1	2	3	4	5	6	7	8	9
1	62%	15%	0%	23%	0%	0%	0%	0%	0%
2	0%	58%	0%	0%	33%	8%	0%	0%	0%
3	0%	0%	62%	0%	0%	31%	0%	0%	8%
4	17%	0%	0%	67%	0%	0%	17%	0%	0%
5	0%	0%	0%	0%	100%	0%	0%	0%	0%
6	0%	0%	0%	0%	0%	44%	0%	0%	56%
7	0%	0%	0%	17%	0%	0%	83%	0%	0%
8	0%	0%	0%	8%	0%	0%	58%	33%	0%
9	0%	0%	0%	0%	0%	8%	0%	0%	92%

Palm16 (Avg. 99%)

FEMALE Responses

stimuli	1	2	3	4	5	6	7	8	9
1	100%	0%	0%	0%	0%	0%	0%	0%	0%
2	0%	100%	0%	0%	0%	0%	0%	0%	0%
3	0%	0%	100%	0%	0%	0%	0%	0%	0%
4	0%	0%	0%	92%	8%	0%	0%	0%	0%
5	0%	0%	0%	0%	100%	0%	0%	0%	0%
6	0%	0%	0%	0%	0%	100%	0%	0%	0%
7	0%	0%	0%	0%	0%	0%	100%	0%	0%
8	0%	0%	0%	0%	0%	0%	0%	100%	0%
9	0%	0%	0%	0%	0%	0%	0%	0%	100%

Palm 16 (Avg. 71%)

MALE Responses

stimuli	1	2	3	4	5	6	7	8	9
1	100%	0%	0%	0%	0%	0%	0%	0%	0%
2	0%	67%	8%	0%	25%	0%	0%	0%	0%
3	0%	0%	50%	0%	0%	33%	0%	0%	17%
4	8%	0%	0%	92%	0%	0%	0%	0%	0%
5	0%	0%	0%	8%	83%	0%	0%	8%	0%
6	0%	0%	6%	0%	0%	56%	0%	0%	38%
7	0%	0%	0%	25%	0%	8%	67%	0%	0%
8	0%	0%	0%	0%	0%	0%	42%	50%	8%
9	0%	0%	0%	0%	0%	17%	0%	8%	75%

Arm 8 (Avg. 55%)

FEMALE Responses

stimuli	1	2	3	4	5	6	7	8	9
1	62%	0%	0%	15%	15%	0%	8%	0%	0%
2	0%	42%	0%	17%	42%	0%	0%	0%	0%
3	0%	0%	54%	0%	8%	31%	0%	0%	8%
4	33%	0%	0%	42%	0%	0%	25%	0%	0%
5	8%	0%	0%	8%	50%	0%	8%	25%	0%
6	0%	0%	0%	0%	11%	56%	0%	11%	22%
7	0%	0%	0%	15%	0%	0%	85%	0%	0%
8	0%	0%	0%	8%	25%	0%	17%	42%	8%
9	0%	0%	0%	0%	0%	17%	0%	17%	67%

Arm 8 (Avg. 35%)

MALE Responses

stimuli	1	2	3	4	5	6	7	8	9
1	67%	8%	0%	17%	0%	0%	8%	0%	0%
2	17%	8%	8%	0%	25%	0%	17%	17%	8%
3	0%	0%	11%	11%	22%	22%	0%	11%	22%
4	8%	17%	0%	42%	17%	0%	8%	8%	0%
5	8%	25%	8%	8%	17%	8%	8%	8%	8%
6	0%	0%	8%	0%	17%	17%	0%	25%	33%
7	0%	0%	0%	8%	8%	0%	83%	0%	0%
8	0%	0%	0%	17%	8%	17%	8%	42%	8%
9	0%	17%	0%	0%	17%	8%	8%	25%	25%

Arm 16 (Avg. 67%)

FEMALE Responses

stimuli	1	2	3	4	5	6	7	8	9
1	69%	8%	0%	23%	0%	0%	0%	0%	0%
2	8%	58%	0%	0%	25%	0%	0%	8%	0%
3	0%	0%	62%	0%	8%	23%	0%	0%	8%
4	25%	0%	0%	75%	0%	0%	0%	0%	0%
5	0%	17%	0%	8%	42%	17%	8%	8%	0%
6	0%	0%	30%	0%	0%	50%	0%	0%	20%
7	0%	0%	0%	15%	0%	0%	85%	0%	0%
8	0%	0%	0%	0%	17%	0%	25%	58%	0%
9	0%	0%	0%	0%	0%	0%	0%	0%	100%

Arm 16 (Avg. 39%)

MALE Responses

stimuli	1	2	3	4	5	6	7	8	9
1	50%	8%	0%	25%	8%	8%	0%	0%	0%
2	17%	17%	8%	8%	42%	8%	0%	0%	0%
3	0%	0%	22%	0%	0%	44%	0%	0%	33%
4	25%	25%	0%	25%	0%	0%	25%	0%	0%
5	0%	0%	8%	0%	23%	38%	0%	15%	15%
6	0%	0%	0%	0%	0%	56%	0%	0%	44%
7	0%	0%	0%	33%	0%	0%	58%	0%	8%
8	0%	8%	8%	0%	0%	8%	17%	50%	8%
9	0%	0%	0%	0%	0%	17%	0%	33%	50%

Thigh 8 (Avg. 52%)

FEMALE Responses

stimuli	1	2	3	4	5	6	7	8	9
1	69%	8%	0%	23%	0%	0%	0%	0%	0%
2	23%	54%	15%	0%	8%	0%	0%	0%	0%
3	0%	8%	75%	0%	0%	17%	0%	0%	0%
4	31%	15%	0%	38%	0%	0%	8%	8%	0%
5	0%	0%	0%	0%	75%	0%	8%	8%	8%
6	0%	0%	11%	0%	11%	56%	0%	11%	11%
7	0%	0%	0%	55%	0%	0%	36%	0%	9%
8	0%	0%	8%	17%	8%	17%	8%	42%	0%
9	0%	0%	0%	0%	8%	25%	0%	42%	25%

Thigh 8 (Avg. 43%)

MALE Responses

stimuli	1	2	3	4	5	6	7	8	9
1	58%	17%	0%	25%	0%	0%	0%	0%	0%
2	15%	54%	15%	8%	0%	8%	0%	0%	0%
3	0%	0%	67%	0%	0%	33%	0%	0%	0%
4	25%	8%	8%	33%	8%	0%	8%	8%	0%
5	8%	31%	8%	8%	15%	0%	15%	15%	0%
6	0%	0%	0%	0%	11%	33%	22%	11%	22%
7	15%	0%	0%	0%	8%	0%	69%	8%	0%
8	0%	0%	0%	0%	8%	15%	46%	23%	8%
9	0%	0%	0%	0%	33%	17%	8%	8%	33%

Thigh 16 (Avg. 47%)

FEMALE Responses

stimuli	1	2	3	4	5	6	7	8	9
1	92%	8%	0%	0%	0%	0%	0%	0%	0%
2	8%	67%	25%	0%	0%	0%	0%	0%	0%
3	0%	0%	83%	0%	0%	17%	0%	0%	0%
4	62%	0%	0%	31%	8%	0%	0%	0%	0%
5	0%	38%	23%	8%	31%	0%	0%	0%	0%
6	0%	0%	22%	0%	33%	33%	0%	0%	11%
7	7%	0%	0%	57%	7%	0%	29%	0%	0%
8	0%	0%	0%	10%	70%	10%	0%	10%	0%
9	0%	0%	0%	0%	0%	31%	0%	23%	46%

Thigh 16 (Avg. 39%)

MALE Responses

stimuli	1	2	3	4	5	6	7	8	9
1	33%	17%	0%	33%	0%	0%	17%	0%	0%
2	0%	54%	31%	0%	8%	0%	8%	0%	0%
3	0%	0%	56%	0%	0%	22%	0%	0%	22%
4	42%	8%	0%	33%	17%	0%	0%	0%	0%
5	0%	23%	8%	23%	31%	8%	0%	0%	8%
6	11%	0%	11%	0%	11%	33%	0%	0%	33%
7	0%	0%	0%	50%	8%	0%	42%	0%	0%
8	0%	8%	0%	8%	25%	0%	25%	17%	17%
9	0%	0%	0%	8%	15%	15%	0%	8%	54%

Appendix 4. Information Transfer (IT) values

Palm 8

IT = 2.3439

	1	2	3	4	5	6	7	8	9
1	2.9456	0.5951	0	0.2903	0	0	0	0	0
2	0	2.8764	0	0	1.3264	-1.236	0	0	0
3	0	0	2.963	0	0	1.4561	0	0	-1.817
4	-0.224	0	0	2.6826	0	0	-0.902	0	0
5	0	0	0	0	2.7415	0	0	0	0
6	0	0	-0.676	0	0	2.7642	0	0	1.0355
7	0	0	0	-0.71	0	0	2.6212	0	0
8	0	0	0	-1.651	0	0	0.9639	3.1565	0
9	0	0	0	0	0	-1.236	0	0	2.8221

Palm 16

IT = 2.4563

	1	2	3	4	5	6	7	8	9
1	3.1177	0	0	0	0	0	0	0	0
2	0	3.1766	-0.911	0	0.0611	0	0	0	0
3	0	0	3.1887	0	0	0.7254	0	0	-0.585
4	-1.526	0	0	2.8864	-1.583	0	0	0	0
5	0	0	0	-1.578	2.9356	0	0	-1.216	0
6	0	0	-0.97	0	0	2.6438	0	0	0.7485
7	0	0	0	0.0067	0	-1.467	2.8547	0	0
8	0	0	0	0	0	0	0.7958	2.9733	-1.837
9	0	0	0	0	0	-0.526	0	-1.275	2.6229

Arm 8

IT = 1.0153

	1	2	3	4	5	6	7	8	9
1	2.447	-0.717	0	0.447	-0.954	0	-1.038	0	0
2	-0.494	1.9274	-0.31	-0.494	1.1054	0	-0.98	-0.605	-1.435
3	0	0	2.8158	-1.369	-0.184	1.6123	0	-1.48	0.2753
4	0.8278	0.3424	0	1.8278	-0.895	0	0.0205	-1.605	0
5	-0.494	0.9274	-0.31	-0.494	1.1054	-1.098	-0.98	0.3949	-1.435
6	0	0	-0.117	0	-0.117	1.9018	0	0.5875	1.3424
7	0	0	0	0.032	-1.954	0	2.3539	0	0
8	0	0	0	0.0909	0.1054	-0.098	-0.395	1.7168	-0.435
9	0	0.3424	0	0	-0.895	0.4868	-1.98	0.7168	2.0242

Arm 16

IT = 1.4246

	1	2	3	4	5	6	7	8	9
1	2.3992	-0.01	0	0.9618	-1.245	-1.781	0	0	0
2	0.1361	2.2186	-0.864	-1.564	1.8142	-1.722	0	-1.256	0
3	0	0	2.5836	0	-1.06	1.211	0	0	0.3075
4	1.1361	0.6336	0	2.0207	0	0	-0.034	0	0
5	0	-0.01	-0.923	-1.623	1.7553	1.0266	-1.678	0.2699	-0.877
6	0	0	1.0581	0	0	1.9371	0	0	1.1039
7	0	0	0	0.9618	0	0	2.4923	0	-1.877
8	0	-0.951	-0.864	0	-0.186	-1.722	0.7032	2.4443	-1.818
9	0	0	0	0	0	-0.66	0	0.8052	2.3308

Thigh 8

IT = 1.1695

	1	2	3	4	5	6	7	8	9
1	2.1367	0.032	0	1.032	0	0	0	0	0
2	0.402	2.1978	0.5107	-1.61	-1.489	-1.489	0	0	0
3	0	-1.302	2.7257	0	0	1.1408	0	0	0
4	0.944	0.032	-1.433	1.6169	-1.433	0	-0.717	-0.369	0
5	-1.863	0.447	-1.433	-1.553	2.0267	0	-0.132	0.2164	-0.61
6	0	0	-0.959	0	0.0412	2.0412	-0.243	0.1054	1.4493
7	-0.804	0	0	1.0909	-1.374	0	2.0428	-1.31	-0.551
8	0	0	-1.433	-0.553	-0.433	0.5673	1.0909	1.6314	-0.61
9	0	0	0	0	0.9481	0.9481	-1.658	1.2753	2.2567

Thigh 16

IT = 1.3173

	1	2	3	4	5	6	7	8	9
1	2.1024	-0.073	0	0.1054	0	0	0.2429	0	0
2	-1.863	2.1904	1.0402	0	-1.816	0	-0.816	0	0
3	0	0	2.3913	0	0	1.1725	0	0	-0.117
4	1.8371	-1.717	0	1.0465	-0.231	0	0	0	0
5	0	1.2269	0.1763	-0.01	1.1274	-1.136	0	0	-1.425
6	-1.389	0	0.2918	0	0.6579	1.9798	0	0	1.1054
7	-1.92	0	0	1.7972	-0.873	0	2.2973	0	0
8	0	-1.532	0	-0.769	1.6903	-0.895	0.9533	2.0529	-0.184
9	0	0	0	-2.01	-0.873	1.4493	0	2.2269	2.2753

Male vs. Female (IT)	Palm		Arm		Thigh		TOTAL
	8	16	8	16	8	16	
Female	2.81	3.11	1.58	1.95	1.51	1.71	1.73
Male	2.11	2.14	0.90	1.30	1.19	1.18	1.09